

Article

Paleoproterozoic Pt-Pd Fedorovo-Pansky and Cu-Ni-Cr Monchegorsk Ore Complexes: Age, Metamorphism, and Crustal Contamination According to Sm-Nd Data

Pavel A. Serov 

Geological Institute of the Kola Science Centre, Russian Academy of Sciences, 184209 Apatity, Russia; serov@geoksc.apatity.ru

Abstract: This paper continues the Sm-Nd isotope geochronological research carried out at the two largest Paleoproterozoic ore complexes of the northeastern Baltic Shield, i.e., the Cu-Ni-Cr Monchegorsk and the Pt-Pd Fedorovo-Pansky intrusions. These economically significant deposits are examples of layered complexes in the northeastern part of the Fennoscandian Shield. Understanding the stages of their formation and transformation helps in the reconstruction of the long-term evolution of ore-forming systems. This knowledge is necessary for subsequent critical metallogenic and geodynamic conclusions. We applied the Sm-Nd method of comprehensive age determination to define the main age ranges of intrusion. Syngenetic ore genesis occurred 2.53–2.85 Ga; hydrothermal metasomatic ore formation took place 2.70 Ga; and the injection of additional magma batches occurred 2.44–2.50 Ga. The rock transformation and redeposited ore formation at 2.0–1.9 Ga corresponded to the beginning of the Svecofennian events, widely presented on the Fennoscandian Shield. According to geochronological and Nd-Sr isotope data, rocks of the Monchegorsk and the Fedorovo-Pansky complexes seemed to have an anomalous mantle source in common with Paleoproterozoic layered intrusions of the Fennoscandian Shield (enriched with lithophile elements, ϵNd values vary from -3.0 to $+2.5$ and ISr 0.702–0.705). The data obtained comply with the known isotope-geochemical and geochronological characteristics of ore-bearing layered intrusions in the northeastern Baltic Shield. An interaction model of parental melts of the Fennoscandian layered intrusions and crustal matter shows a small level of contamination within the usual range of 5–10%. However, the margins of the Monchetundra massif indicate a much higher level of crustal contamination caused by active interaction of parental magmas and host rock.



Citation: Serov, P.A. Paleoproterozoic Pt-Pd Fedorovo-Pansky and Cu-Ni-Cr Monchegorsk Ore Complexes: Age, Metamorphism, and Crustal Contamination According to Sm-Nd Data. *Minerals* **2021**, *11*, 1410. <https://doi.org/10.3390/min11121410>

Academic Editor: Federica Zaccarini

Received: 22 November 2021

Accepted: 10 December 2021

Published: 13 December 2021

Keywords: Fennoscandian Shield; Arctic region; Cu-Ni-PGE ores; mafic-ultramafic complexes; metallogeny; layered intrusions; ore magmatic system; geochronology; Sm-Nd; crustal contamination; isotope methods

Publisher's Note: MDPI stays neutral with regard to jurisdictional claims in published maps and institutional affiliations.



Copyright: © 2021 by the author. Licensee MDPI, Basel, Switzerland. This article is an open access article distributed under the terms and conditions of the Creative Commons Attribution (CC BY) license (<https://creativecommons.org/licenses/by/4.0/>).

1. Introduction

The Russian Arctic zone provides high investment opportunities, particular regarding the large mining operations on the Fennoscandian ore deposits. Industrial concerns, as well as securing growth (of the potential capacity) of ore deposits are major issues. To solve them, we should determine the ore matter concentrating patterns. In the northeastern Baltic Shield, large-scale mafic-ultramafic deposits of Cu-Ni, platinum group elements (PGE), and Fe-Ti-V are economically significant, particularly concerning critical raw materials, such as PGE and V. There are major Cu-Ni-Cr+(PGE) deposits in the Monchegorsk ore district [1–5] and Pechenga [6–8], Fe-Ti-V Kolvitsa deposit [9,10], PGE Fedorovo-Pansky layered complex [11–15], Burakovsky intrusion [16], Cu-Ni-Co (+PGE) deposits in Finland: Kemi [5,17], Penikat [18,19], Akanvaara, Koitelainen [20], Tornio [21], and so forth. The greatest density of layered intrusions is found in the Fennoscandian Shield, referred to as “Europe’s Treasure Chest” by Maier and Hanski [2], including the Archean Kola and Karelia cratons [22]. The dated deposits were formed in two major episodes, at 2.53–2.39 Ga and

2.0–1.8 Ga, corresponding to the early [5,16,17,23–39] and late [8,40] stages of rifting in the Fennoscandian Shield.

Kola Peninsula deposits, such as Monchetundra, Monchepluton, Main Ridge, and the Fedorovo-Pansky complex, belong to the largest European layered intrusions (the full list of intrusions includes more than 140 items [22]). These ore districts of high economic importance have drawn the attention of scientists for quite some time. A long-term multi-disciplinary study of the Monchegorsk and Fedorovo-Pansky ore complexes is underway. However, some issues remain enigmatic, i.e., the aspects of genesis, timing and duration of formation, transformation processes, sources of ore metals, and the peculiarities of mantle-crust interactions between parental mafic-ultramafic magmas and crustal matter. Studies using the Sm-Nd systematics have made it possible to successfully characterize some geochronological stages of the formation of these deposits [11,13,31,37], but more detailed research is needed.

This article primarily addresses the Sm-Nd geochronological explanation of major events during the formation and transformation (metamorphism) of the largest intrusive complexes, i.e., Monchegorsk and the Fedorovo-Pansky. Geochronological and Nd-Sr isotope data give us the ground to discuss possible sources of melt and interaction between intrusive parental magma and crustal hosts. We also substantiate the importance of additional magma injections into the solidifying horizons of layered complexes.

2. Geological Setting

The Fennoscandian Shield hosts the vast Paleoproterozoic East Scandinavian Mafic Large Igneous province. Its current remnants cover about 1,000,000 km². The shield basement was formed as a mature Archaean granulite and gneiss-migmatite crust 2550 Ma ago. It is exposed in the Kola-Lapland-Karelia Craton. The main structural features of the East Scandinavian Mafic Large Igneous province and its Pd-Pt and Ni-Cu-PGE deposits are described in [41]. The exposed part of the shield extends beneath the sedimentary cover toward the Northern Russian Platform as a vast Paleoproterozoic Baltic-Mid-Russia wide arc-intracontinental orogens [42].

The long Early Paleoproterozoic (2530–2400 Ma) geological history of the East Scandinavian Mafic Large Igneous province comprises several stages. They are separated by breaks in sedimentation and magmatic activity, often marked by uplift erosion and the deposition of conglomerates. The Sumian stage (2550–2400 Ma) is crucial for the metallogeny of Pd-Pt ores. It can be related to the emplacement of high-Mg and high-Si boninite-like and anorthosite magmas [43,44]. The ore-bearing intrusions were emplaced in the Kola Belt and in the Fenno-Karelian Belt [12,13]. The Monchegorsk and the Fedorovo-Pansky complexes are situated in the central part of the Kola Intrusive Belt (Figure 1).

2.1. The Fedorovo-Pansky Layered Complex

The Fedorovo-Pansky Layered Complex crops out over an area of >400 km². It strikes north-west for >60 km and dips southwestward at an angle of 30°–35°. The total rock sequence is about 3–4 km thick. Tectonic faults divide the complex into several blocks (Figure 2). The major blocks from west to east are known as the Fedorova Tundra, Lastjavr, Western, and Eastern Pansky [13,43].

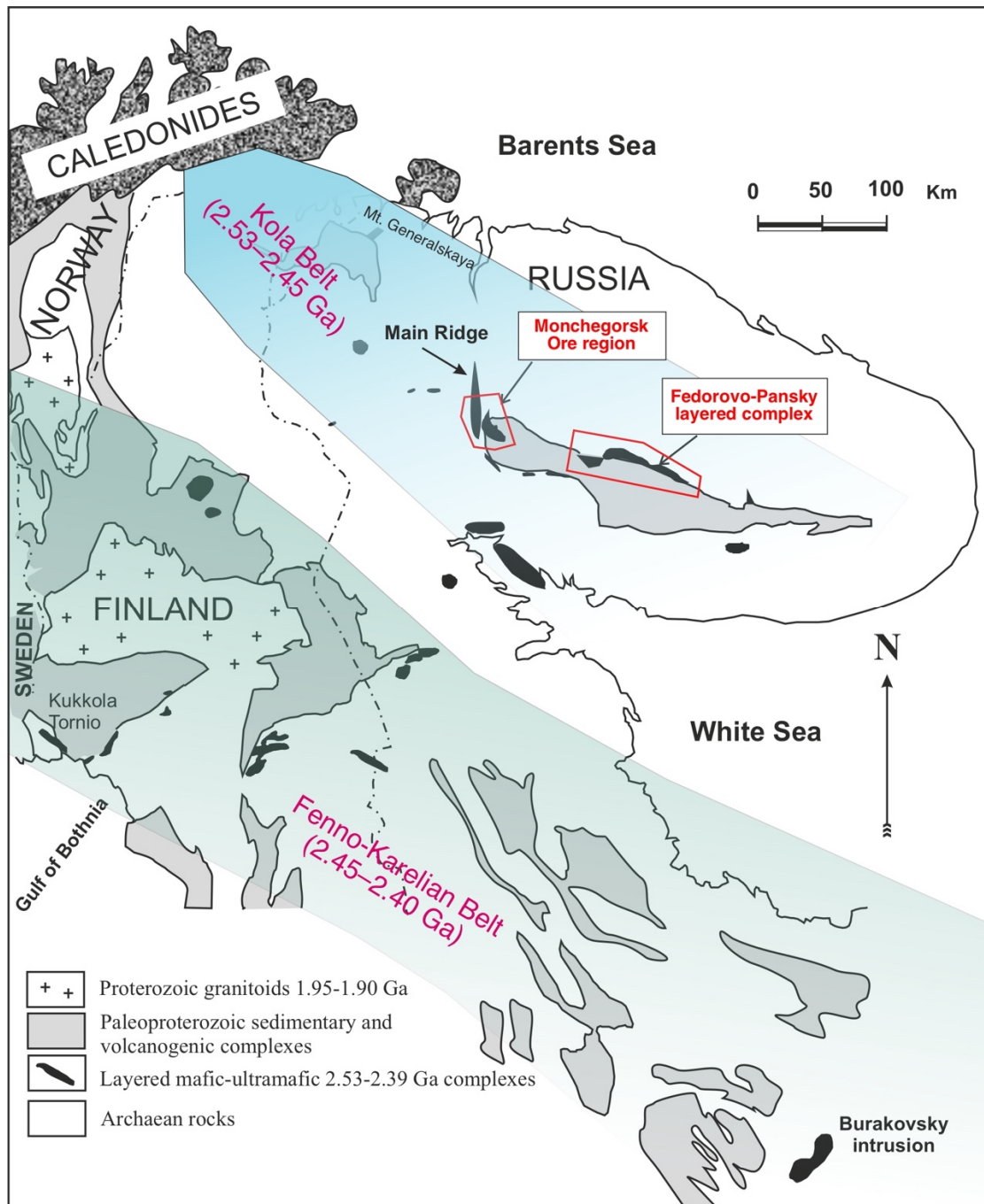


Figure 1. Schematic geological map of the northeastern part of the Fennoscandian Shield and the location of Paleoproterozoic mafic-layered intrusions (modified after [12]). The red frames show the studied ore areas.

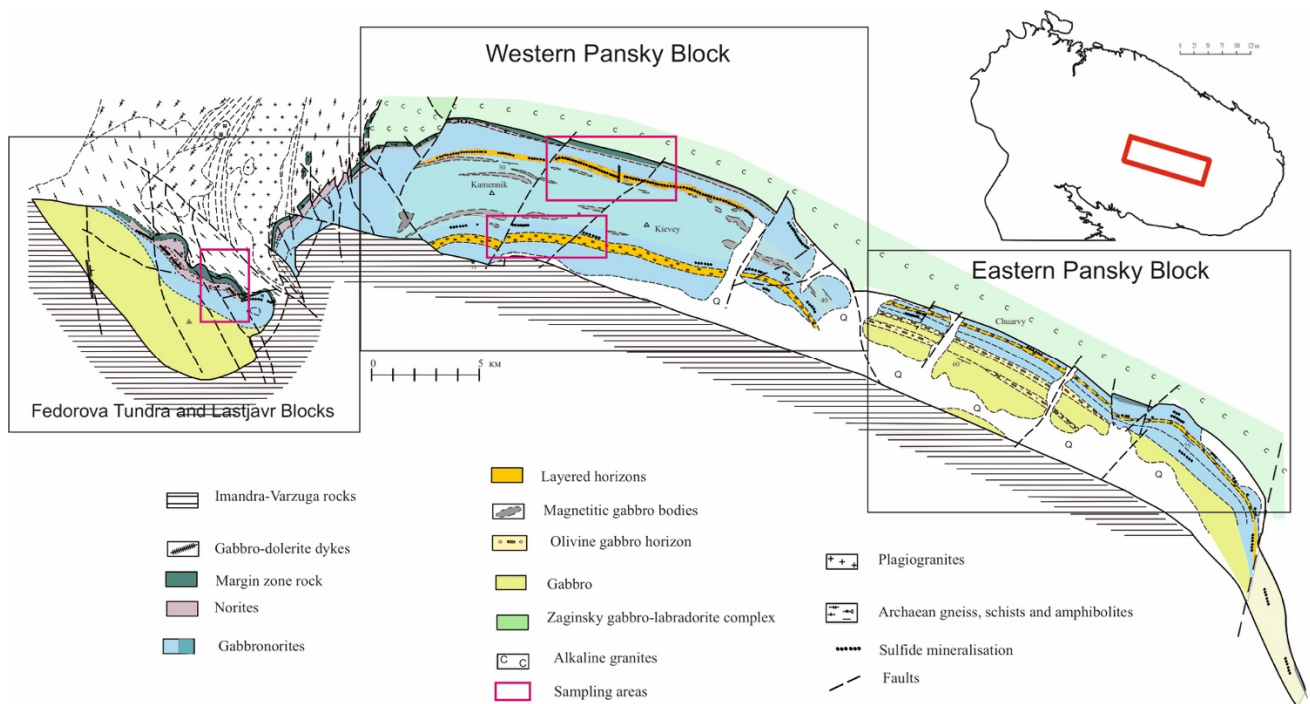


Figure 2. General geological map of the Fedorovo-Pansky Layered Complex (after [43], with author modifications).

The Fedorovo-Pansky complex is bordered by the Paleoproterozoic Imandra-Varzuga rift and Archaean Keivy terrain. The rocks of the complex crop out close to the Archaean gneisses only in the NW extremities, but their contacts cannot be defined because of their poor exposure. In the north, the complex borders alkaline granites of the White Tundra intrusion. The alkaline granites were found to be Archaean with a U-Pb zircon age of $2654 \pm 15\text{Ma}$ [24,45]. The contact of the Western Pansky block with the Imandra-Varzuga volcano-sedimentary sequence is mostly covered by Quaternary deposits. However, drilling and excavations to the south of Mt. Kamennik reveal a strongly sheared and metamorphosed contact between the intrusion and overlying Paleoproterozoic volcano-sedimentary rocks that we consider tectonic. The Fedorovo-Pansky complex mostly comprises gabbronorites [12,14]. From the bottom up, the layered sequence is as follows:

1. Marginal zone (50–100 m) of plagioclase-amphibole schists with relicts of norite and gabbronorite, which are referred to as chilled margin rocks.
2. Taxitic zone (30–300 m), which contains an ore-bearing gabbronoritic matrix and early xenoliths of norite and pyroxenite. Syngenetic ores are represented by Cu and Ni sulfides with Pt, Pd, and Au.
3. Norite zone (50–200 m) with cumulus interlayers of harzburgite and pyroxenite that include an intergranular injection Cu-Ni-PGE mineralization in the lower part. The rocks of this zone are enriched in chromium (up to 1000 ppm), and contain chromite.
4. Main Gabbronorite zone (about 1000 m) is a thickly layered “stratified” rock series with a 40–80 m thinly layered lower horizon (LLH) in the upper part. LLH consists of contrasting alteration of gabbronorite, norite, pyroxenite, and interlayers of leucocratic gabbro and anorthosites. LLH contains a reef-type PGE deposit poor in base-metal sulfides. The upper-layered horizon (ULH) is positioned between the lower and upper Gabbro zones. ULH consists of olivine-bearing troctolite, norite, gabbronorite, and anorthosite. The U-Pb age of the ULH rocks on zircon and baddeleyite is $2447 \pm 12\text{Ma}$ [24]. It is the youngest age among those obtained for the Fedorovo-Pansky Complex rocks [24,35]. Yet, recent analyses based on studies of a drill sample from boreholes and the U-Pb study of zircons using the SHRIMP-II allowed determining a more ancient age of the ULH anorthosites, i.e., $2509.4 \pm 6.2\text{Ma}$ [46].

2.2. Monchegorsk Complex of Layered Intrusions

The Monchegorsk mafic-ultramafic pluton (Monchepluton) and the substantially mafic Monchetundra massif compose the Monchegorsk Complex of layered intrusions [4,37,44,47].

The Monchepluton is located in the central Kola Peninsula at the NW edge of the Paleoproterozoic Imandra-Varzuga volcanic-sedimentary rift structure. Currently, the pluton is arc shaped and consists of two branches (chambers). The NW branch is more than 7 km in length and comprises the Nittis-Kumuzhya-Travyanaya (NKT) deposit. The nearly latitudinal branch is about 11 km in length and consists of the Sopcha-Nyud-Poaz and Vurechuayvench massifs (Figure 3).

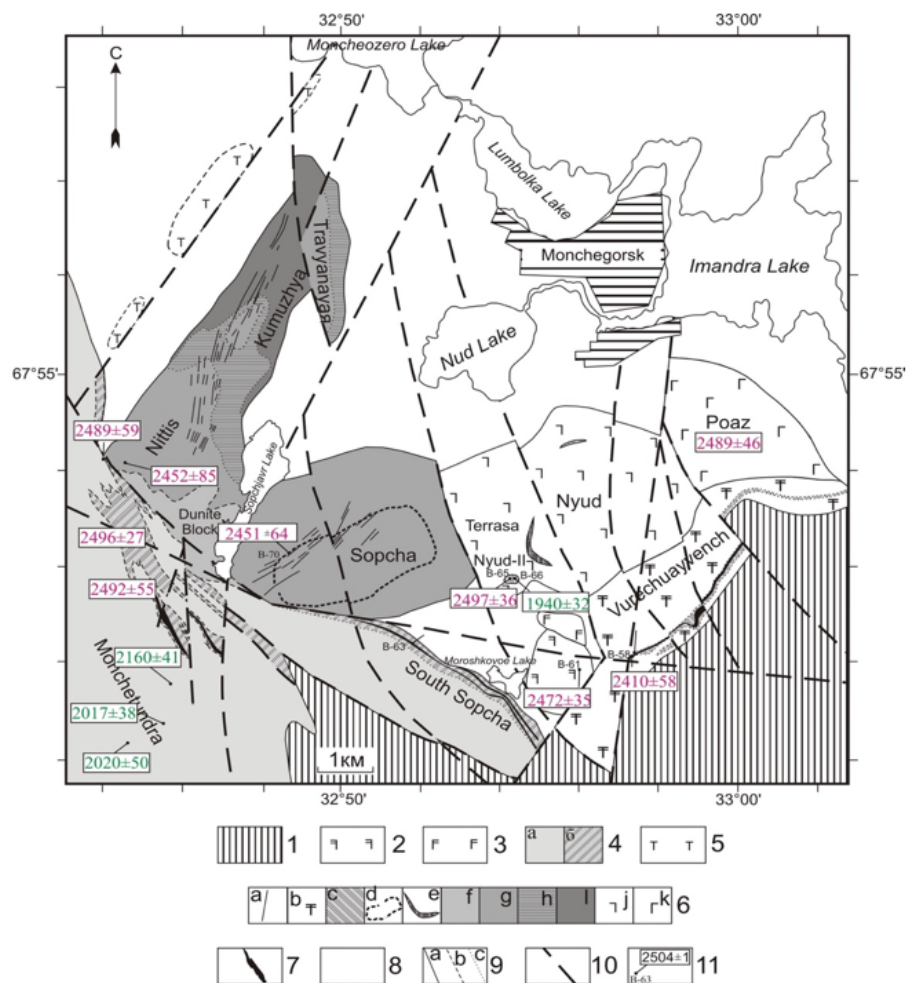


Figure 3. General geological map of Monchegorsk region with results of Sm-Nd geochronological studies (modified after [37]). Paleoproterozoic formations (1–6): 1—Imandra-Varzuga volcanic-sedimentary riftogenic structure; 2—metagabbro and metanorite of Lake Moroshkovoe massif; 3—quartz metagabbro of “10 anomaly” massif; 4—Monchetundra massif: (a) leucocratic metagabbro, metagabbro and anorthosites from upper zone and (b) metanorites and metaorthopyroxenites from the lower zone; (5) gabbro of Kirikha massif; (6) Monchepluton: (a) sulfide veins, (b) “330 horizon” of Sopcha, (c) metagabbro (d) metaplagioclases of Vurechuayvench massif, (e) Nyud “critical horizon”, (f) gabbro, (g) norite, (h) orthopyroxenite, (i) orthopyroxenite and harzburgite interbedding, (j) harzburgite, (k) dunite block; (7) horizons of low-sulfide PGE mineralization; (8) Archean metamorphic formations of Kola Block; (9) geological boundaries: reliable, (b) inferred, (c) facies; (10) faults; (11) location of samples, their numbers and results of dating.

The pluton is differentiated in the vertical and horizontal directions; that is, the rocks become less basic from the bottom up and from west to east. Dunite, harzburgite, orthopyroxenites (NKT), orthopyroxenites (Sopcha), norites (Nyud), and gabbro-norites (Poaz, Vurechuayvench) make up a common syngenetic series of rocks [37,48]. In the upper part, a continuous orthopyroxenite body of the Sopcha massif is disturbed by Horizon 330. "Horizon 330" is considered to originate as an injection of an additional magma batch [37]. It is more basic and has higher temperature than the initial melt in the magma chamber [4,37,49]. The horizon is characterized by a rhythmic sequence of thin (10–130 cm) layers composed of dunites, harzburgites, olivine orthopyroxenites, and feldspathic orthopyroxenites [37,48,49]. The layering is disturbed by bends and folds formed as a result of melt flow [37].

3. Samples and Methods

The isotope research was carried out at the Collective Use Centre of the Kola Science Centre RAS (Apatity, Russia). First, the samples were prepared by crushing; then, minerals were separated using heavy liquids, and mineral fractions were selected under binocular microscope.

3.1. Sm-Nd Analytical Methods

In order to define concentrations of Sm and Nd, the sample was mixed with a compound ^{149}Sm - ^{150}Nd tracer prior to dissolution. Then, it was dissolved with a mixture of HF + HNO₃ (or + HClO₄) in Teflon sample bottles at a temperature of 100 °C until complete dissolution. Further extraction of Sm and Nd was carried out using standard procedures with two-stage ion-exchange and extraction-chromatographic separation using ion-exchange resin "Dowex" 50 × 8 in chromatographic columns employing 2.3 N and 4.5 N HCl as an eluent. The separated Sm and Nd fractions were transferred into a nitrate form, whereupon the samples (preparations) were ready for mass-spectrometric analysis.

The Nd isotope composition and Sm and Nd contents were measured with a 7-channel solid-phase mass-spectrometer Finnigan-MAT 262 (RPQ) in a static double-band mode, using Ta + Re filaments. The mean value of $^{143}\text{Nd}/^{144}\text{Nd}$ ratio in a JNd_i-1 standard was 0.512081 ± 13 (N = 11) in the test period. Error in $^{147}\text{Sm}/^{144}\text{Nd}$ ratios was 0.3% (2σ), which is a mean value for 7 measurements of BCR-2 standard [50]. The error in estimation of isotope Nd composition in an individual analysis was up to 0.01% for minerals with low Sm and Nd contents. The blank intralaboratory contamination was 0.3 ng of Nd and 0.06 ng of Sm. The accuracy of estimation of Sm and Nd contents was ±0.5%. Isotope ratios were normalized to $^{146}\text{Nd}/^{144}\text{Nd} = 0.7219$ and then recalculated for $^{143}\text{Nd}/^{144}\text{Nd}$ in JNd_i-1 = 0.512115 [51]. Parameters of isochrons were estimated using the ISOPLOT program complex [52]. Values of εNd(T) and T(DM) model ages were estimated using present-day values of CHUR as described in [53] at ($^{143}\text{Nd}/^{144}\text{Nd} = 0.512630$, $^{147}\text{Sm}/^{144}\text{Nd} = 0.1960$) and DM as described in [54] ($^{143}\text{Nd}/^{144}\text{Nd} = 0.513151$, $^{147}\text{Sm}/^{144}\text{Nd} = 0.2136$).

3.2. Samples for Sm-Nd Analyses

Samples for Sm-Nd analysis were taken from the rocks (WR), rock forming, and ore minerals of the Fedorovo-Pansky (Figure 2) and the Monchegorsk (Figure 3) layered complexes.

3.2.1. Fedorovo-Pansky Complex

Rocks of the lower and upper-layered horizons within the Western Pansky block of the intrusive were investigated since major ore districts of the complex are related to these horizons. From the lower layered horizon (LLH), ore gabbro-norites SN-3, H-08-01, FPM-1, MP-1; norite SN-6, and mineralized gabbro H-08-02/1 were sampled for Sm-Nd dating; gabbro-norites H-08-04 and SN-1 and anorthosites H-08-05 were sampled from the Upper Layered Horizon (ULH). Samples were taken in the Fedorova Tundra block from all major areas of the complex (stratigraphically from bottom to top), i.e., taxite, norite, gabbro-norites, and gabbro areas (Figures 2 and 4). From the taxite area, harzburgites (F-1), taxite gabbro-norites (F-2 and FT-2), and plagiopyroxenites (F-3) were sampled; from the

norite area, pyroxenite (FT-1); from the gabbro-norite area, olivine gabbro-norite (FT-3), and gabbro (F-4); from gabbro, gabbro (BGF-616).

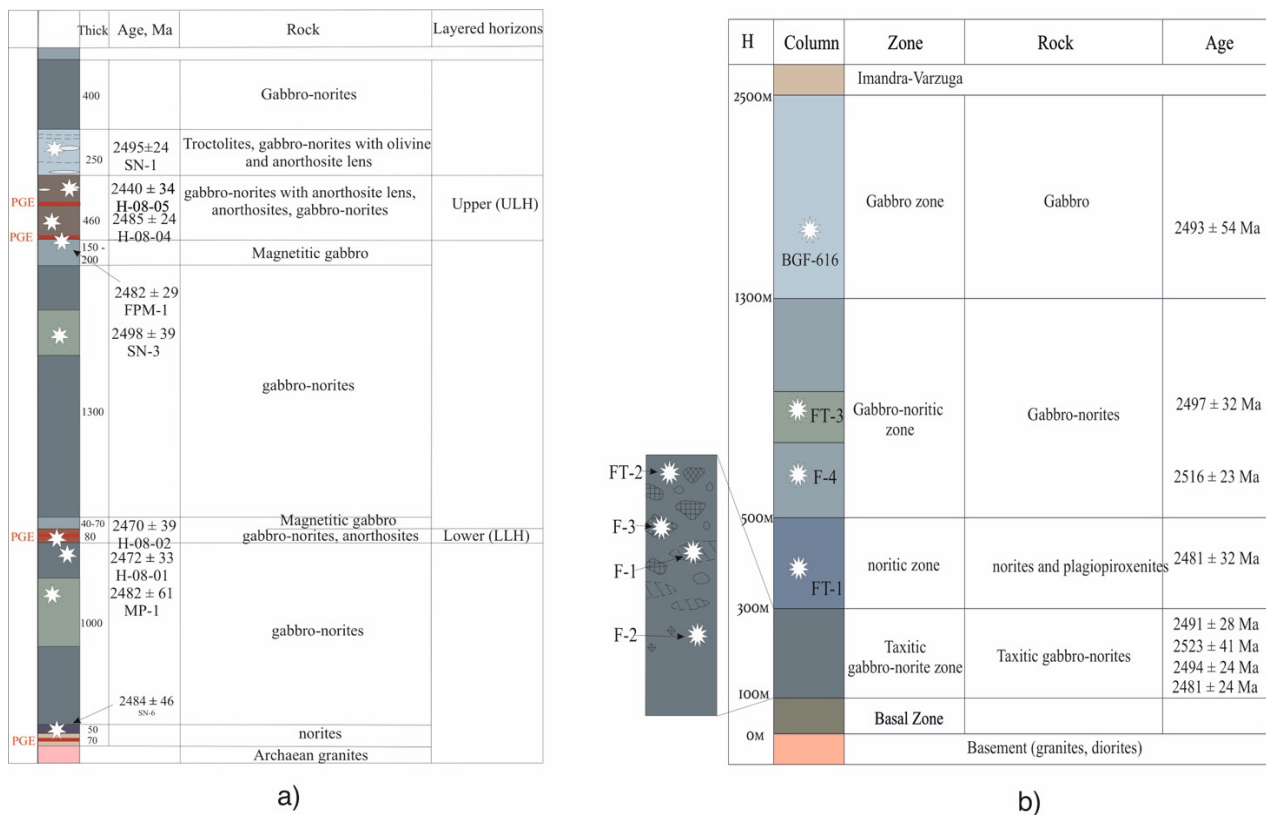


Figure 4. A generalized column for (a) West-Pana and (b) Fedorova Tundra blocks with Sm-Nd results (modified after [11]).

3.2.2. Monchegorsk Complex

Rocks of all main varieties were studied within the Monchegorsk complex (Figure 3). From the Monchepluton complex, the following were sampled: orthopyroxenites and ore-bearing norites of Nyud-II (samples B65/111 and B66/111); harzburgites of the horizon 330 ore layer, Sopcha (sample B70/111); metaplagioclase with sulfides, Vurechuyvench (sample B58/111); gabbro-norites of Moroshkovoe Lake (sample B61/111); gabbro-norite of Poaz (sample 409); orthopyroxenites of Pentlandite Gorge (samples MT-3 and P-1/109). In Monchetundra area were sampled: metaolivinites (sample MT-65), trachitoid gabbro-norites (samples B19/111 and B20/111), leucogabbro-norite (sample 1/106), and gabbro-norite (sample 7/106). In the Sopchezero deposit, dunites (sample 405) and chromitites (sample 404) were collected.

4. Results and Discussion

The results of isotope geochronological research of rocks and minerals from both complexes are summarized in Figures 3 and 4, Tables 1 and 2.

Table 1. Results of isotope Sm-Nd studies of rocks and minerals of the Fedorovo-Pansky Complex.

Sample	Concentrations ppm		Isotopic Ratios		T_{DM} , Ma	$\epsilon_{Nd}(T)$		
	Sm	Nd	$^{147}\text{Sm}/^{144}\text{Nd}$	$^{143}\text{Nd}/^{144}\text{Nd}$				
Fedorova Tundra norite (F-2)								
WR	0.423	1.662	0.1537	0.511807 ± 20	3393	−2.6		
Pl	0.413	2.88	0.0865	0.510709 ± 14				
Cpx	1.777	5.73	0.1876	0.512381 ± 8				
Opx	0.125	0.325	0.2323	0.513085 ± 10				
Fedorova Tundra orthopyroxenite (F-3)								
WR	0.318	1.166	0.1648	0.512196 ± 12	2964	+1.7		
Opx	0.139	0.376	0.2228	0.513172 ± 17				
Cpx	2.21	7.67	0.1745	0.512349 ± 16				
Pl	0.257	1.615	0.0961	0.511071 ± 29				
Gabbro of Fedorova Tundra block (F-4)								
WR	0.629	2.80	0.1357	0.511548 ± 8	3115	−1.6		
Opx	0.233	0.721	0.1951	0.512555 ± 15				
Cpx	0.826	2.28	0.2187	0.512947 ± 16				
Pl	0.239	1.772	0.0815	0.510677 ± 14				
Ol	0.512	1.937	0.1109	0.511141 ± 29				
Gabbronorite (SN-1)								
WR	0.303	1.429	0.1281	0.511377 ± 19	3141	−2.7		
Pl	0.144	0.984	0.0885	0.510739 ± 11				
Cpx	1.478	4.43	0.2015	0.512598 ± 9				
Opx	0.200	0.553	0.2183	0.512870 ± 11				
Marginal Zone norite (SN-6)								
WR	0.311	1.575	0.1003	0.511039 ± 10	2824	−0.5		
Cpx	2.42	8.84	0.1657	0.512119 ± 20				
Pl	0.252	1.829	0.0833	0.510790 ± 29				
Opx	0.182	0.672	0.1641	0.512027 ± 20				
Gabbronorite of Malaya Pana (MP-1)								
WR	1.044	4.99	0.1263	0.511441 ± 10	2967	−1.0		
Po	0.029	0.151	0.1144	0.511217 ± 21				
Pn	0.008	0.044	0.1160	0.511259 ± 23				
Pl-2	0.398	2.247	0.0977	0.510957 ± 19				
Pl-1	0.325	2.302	0.0853	0.510738 ± 17				
Opx + Cpx	4.75	16.44	0.1747	0.512203 ± 7				
Cpx + Opx	2.54	9.34	0.1641	0.512033 ± 9				
Ccp + Pn	0.022	0.122	0.1106	0.511143 ± 20				
Ore-bearing gabbronorite of Kievey (FPM-1)								
WR	0.560	3.12	0.1096	0.511125 ± 14	2951	−1.8		
Po	0.030	0.181	0.1050	0.511044 ± 26				
Pn + Py + Ccp	0.429	1.662	0.1521	0.511821 ± 23				
Ccp	0.053	0.251	0.1086	0.511132 ± 20				
Cpx	0.855	4.92	0.1733	0.512174 ± 14				
Opx	1.144	5.07	0.1802	0.512290 ± 11				
Pl	0.212	0.955	0.0844	0.510722 ± 17				
Ore-bearing gabbronorite of Kievey (H-08-01)								
WR	0.999	4.75	0.1271	0.511353 ± 17			3146	−3.0
Cpx + Opx	1.312	4.66	0.1702	0.512055 ± 17				
Opx	0.158	0.467	0.2047	0.512625 ± 22				
Cpx	8.33	30.8	0.1634	0.511954 ± 17				
Ap	194.2	972.4	0.1207	0.511248 ± 15				
Pl	0.145	0.914	0.0961	0.510855 ± 14				

Table 1. Cont.

Sample	Concentrations ppm		Isotopic Ratios		T _{DM} , Ma	ε _{Nd} (T)
	Sm	Nd	¹⁴⁷ Sm/ ¹⁴⁴ Nd	¹⁴³ Nd/ ¹⁴⁴ Nd		
Ore-bearing gabbro of Kievey (H-08-02)						
WR	1.019	5.03	0.1224	0.511355 ± 21	2982	−1.5
Ap	156.5	753.7	0.1255	0.511385 ± 19		
Amf	0.888	4.692	0.1145	0.511239 ± 17		
Cpx	7.35	26.1	0.1700	0.512139 ± 16		
Pl	0.206	1.423	0.0874	0.510792 ± 14		
Gabbronorite of ULH (H-08-04)						
WR	0.409	1.462	0.1011	0.510879 ± 17	3058	−3.9
Cpx	1.072	3.31	0.1957	0.512441 ± 14		
Cpx + Opx	0.299	0.908	0.1992	0.512473 ± 22		
Opx	0.095	0.262	0.2193	0.512801 ± 20		
Pl	0.130	0.889	0.0885	0.510655 ± 19		
Anorthosite of ULH (H-08-05)						
WR	0.271	1.176	0.1393	0.511613 ± 17	3133	−2.1
Pl	0.107	0.719	0.0901	0.510833 ± 21		
Opx	0.921	2.94	0.1896	0.512436 ± 13		
Cpx	0.801	2.99	0.1618	0.511978 ± 11		
Fedorova Tundra pyroxenite (FT-1)						
WR	0.252	0.972	0.1367	0.511608 ± 11	3038	−1.0
Opx + Cpx	0.155	0.522	0.1679	0.512129 ± 13		
Opx	0.139	0.482	0.1740	0.512237 ± 19		
Cpx	3.79	14.47	0.1582	0.511968 ± 17		
Pl	0.200	1.510	0.0800	0.510695 ± 16		
Fedorova Tundra gabbonorite (FT-2)						
WR	0.663	2.70	0.1417	0.511775 ± 16	2899	+0.8
Sulf	0.400	0.267	0.0897	0.510942 ± 18		
Pl	0.179	1.279	0.0846	0.510845 ± 18		
Cpx	2.43	8.49	0.1730	0.512295 ± 14		
Opx	0.230	0.697	0.1996	0.512744 ± 19		
Fedorova Tundra olivine gabbonorite (FT-3)						
WR	1.105	4.76	0.1402	0.511672 ± 14	3051	−0.8
Pl	0.330	1.927	0.1034	0.511275 ± 15		
Ol	0.114	0.539	0.1276	0.511471 ± 16		
Opx	1.125	3.161	0.2151	0.512913 ± 13		
Fedorova Tundra gabbro (BGF-616)						
WR	1.31	5.77	0.1377	0.511727 ± 18	2843	+1.1
Py + Pn	0.08	0.45	0.1089	0.511251 ± 20		
Pn	1.35	7.34	0.1108	0.511283 ± 17		
Pl	1.04	8.31	0.0757	0.510707 ± 14		
Ccp	0.10	0.60	0.1046	0.511165 ± 19		
Py	0.15	0.91	0.1008	0.511130 ± 22		
Gabbronorite, below LLH						
WR	0.642	3.35	0.1159	0.511244 ± 12	2957	−1.3
Zo	0.221	1.859	0.0718	0.510672 ± 21		
Ap	64.2	307.1	0.1209	0.511297 ± 6		
Ore-bearing gabbonorite, LLH						
WR	0.936	4.38	0.1292	0.511484 ± 15	2992	−1.0
Ap-1	149.9	623.3	0.1454	0.511697 ± 5		
Ap-2	58.9	294.4	0.1209	0.511362 ± 6		

WR—whole rock; Pl—plagioclase; Cpx—clinopyroxene; Opx—orthopyroxene; Ol—olivine; Po—pyrrhotite; Pn—pentlandite; Ccp—chalcopyrite; Py—pyrite; Ap—apatite; Zo—zoisite; Amf—amphibole; Sulf—sulfide minerals mix; Gr—garnet; Ilm—ilmenite; Chr—chromite.

Table 2. Sm-Nd data for rocks and minerals of Monchegorsk Complex.

Sample	Concentrations, ppm		Ratios		T _{DM} , Ma	ε _{Nd} (T)
	Sm	Nd	¹⁴⁷ Sm/ ¹⁴⁴ Nd	¹⁴³ Nd/ ¹⁴⁴ Nd ± 2σ		
Orthopyroxenites, Nyud-II, B65/111						
WR	0.456	2.06	0.1333	0.511530 ± 14	3056	−1.2
Sulf	3.39	19.63	0.1043	0.511059 ± 11		
Opx-1	0.039	0.176	0.1355	0.511599 ± 42		
Pl	0.466	5.33	0.0528	0.510218 ± 15		
Opx-2	0.318	1.226	0.1569	0.511961 ± 34		
Ap	158.3	874	0.1094	0.510780 ± 13		
Ore-bearing norites, Nyud-II, B66/111						
Py	0.029	0.168	0.1058	0.511086 ± 13		
Ccp	0.082	0.556	0.0895	0.510842 ± 72		
Opx	1.660	5.69	0.1763	0.511975 ± 16		
Pl	0.272	2.25	0.0731	0.510656 ± 14		
Ap	282	772	0.1148	0.511176 ± 7		
Harzburgite, ore-bed "330", Sopcha, B70/111						
WR	0.043	0.149	0.1656	0.511813 ± 25	—	−6.3
Ol	0.028	0.144	0.1119	0.510982 ± 43		
Sulf	0.034	0.188	0.1106	0.510934 ± 36		
Opx	0.055	0.160	0.2064	0.512499 ± 33		
Plagioclase with sulfides, Vurechuayvench, B58/111						
WR	0.971	4.62	0.1271	0.511408 ± 7	3051	−2.4
Pn	0.109	0.350	0.1884	0.512382 ± 18		
Sulf	0.031	0.116	0.1603	0.511880 ± 87		
Gabbronorite, Moroshkovoe Ozero, B61/111						
WR	0.611	2.95	0.1251	0.511387 ± 13	3017	−1.7
Pl	0.285	1.868	0.0921	0.510867 ± 18		
Opx	0.247	0.699	0.2136	0.512842 ± 45		
Opx + Cpx	0.899	2.98	0.1821	0.512331 ± 18		
Ap	74.6	339.5	0.1328	0.511514 ± 4		
Ru	0.834	5.12	0.0986	0.511307 ± 9		
Gabbronorite, Poaz, 409						
WR	0.897	4.41	0.1229	0.511339 ± 9	3073	−2.4
Opx	0.734	3.07	0.1444	0.511674 ± 21		
Cpx	0.613	1.851	0.2000	0.512595 ± 36		
Pl	0.135	0.861	0.0948	0.510876 ± 14		
Cpx + Opx	0.903	3.06	0.1785	0.512258 ± 20		
Orthopyroxenite, Nittis-Pentlandite Gorge, MT-3						
WR	0.245	1.055	0.1403	0.511815 ± 9	2762	+1.7
Sulf	0.020	0.090	0.1337	0.511703 ± 15		
Pl	0.596	4.94	0.0730	0.510736 ± 12		
Opx	0.156	0.499	0.1892	0.512594 ± 15		
Opx + Ol	0.119	0.371	0.1934	0.512704 ± 25		
Monchetundra metaolivinite, MT-65						
WR	0.081	0.316	0.1546	0.511963 ± 19	—	−1.5
Ol + Opx	0.058	0.263	0.1323	0.511642 ± 24		
Pl	0.565	4.57	0.0747	0.510831 ± 24		
Opx	0.547	1.982	0.1670	0.512152 ± 7		
Ol	0.015	0.093	0.0988	0.511183 ± 20		
Pentlandite Gorge orthopyroxenite, P-1/109						
WR	0.678	2.090	0.1762	0.512377 ± 19	3130	+1.3
Po	0.018	0.095	0.1171	0.511381 ± 59		
Sulf	0.032	0.123	0.1561	0.512015 ± 43		
Cpx	1.048	3.230	0.1961	0.512687 ± 33		
Opx + Cpx	1.095	3.37	0.1902	0.512586 ± 16		
Pl	0.090	0.523	0.1036	0.511171 ± 26		

Table 2. Cont.

Sample	Concentrations, ppm		Ratios		T_{DM} , Ma	$\epsilon_{Nd}(T)$
	Sm	Nd	$^{147}\text{Sm}/^{144}\text{Nd}$	$^{143}\text{Nd}/^{144}\text{Nd} \pm 2\sigma$		
Monchetundra trachitoid gabbronorite, B19/111						
WR	0.462	1.715	0.1628	0.511989 ± 18	3285	−1.6
Pl-1	0.439	2.95	0.0902	0.510801 ± 10		
Pl-2	0.516	3.43	0.0911	0.510823 ± 20		
Cpx	2.94	9.54	0.1862	0.512392 ± 13		
Opx	0.231	0.674	0.2071	0.512723 ± 24		
Monchetundra trachitoid leucogabbronorite, B20/111						
WR	0.870	3.65	0.1441	0.511894 ± 7	2742	−1.7
Pl-1	0.221	1.227	0.1087	0.511323 ± 26		
Pl-2	0.144	0.885	0.0987	0.511164 ± 33		
Opx	0.330	1.143	0.1744	0.512403 ± 32		
Cpx	3.62	12.49	0.1750	0.512413 ± 9		
Dunite, Dunite block (Sopchezero Deposit), 404						
WR	0.622	0.912	0.1243	0.511563 ± 33	2696	+2.5
Cpx	2.95	9.93	0.1797	0.512466 ± 14		
Opx + Cpx	2.45	8.43	0.1756	0.512422 ± 11		
Ol	0.025	0.156	0.0971	0.511119 ± 34		
Chr	2.74	18.23	0.1118	0.511361 ± 10		
Chromitite, Dunite block (Sopchezero Deposit), 405						
WR	3.08	21.5	0.0867	0.510977 ± 12	2598	+2.9
Pl	0.325	3.05	0.0644	0.510635 ± 15		
Ol	0.092	0.357	0.0691	0.510689 ± 17		
Ol + Cpx	0.298	1.202	0.1497	0.512018 ± 11		
Chr	2.87	18.04	0.0914	0.511053 ± 16		
Monchetundra leucogabbronorite, 1/106						
Pl	1.647	9.11	0.1093	0.511355 ± 25		
Gr	1.174	4.24	0.1672	0.512132 ± 23		
Ilm	0.609	3.23	0.1139	0.511430 ± 25		
Monchetundra gabbronorite, 7/106						
Pl	0.016	0.092	0.1051	0.511028 ± 56		
Ilm + Gr	0.035	0.156	0.1352	0.511435 ± 46		
Gr	0.040	0.129	0.1886	0.512138 ± 13		

WR—whole rock; Pl—plagioclase; Cpx—clinopyroxene; Opx—orthopyroxene; Ol—olivine; Po—pyrrhotite; Pn—pentlandite; Ccp—chalcopyrite; Py—pyrite; Ap—apatite; Amf—amphibole; Sulf—sulfide minerals mix; Gr—garnet; Ilm—ilmenite; Chr—chromite.

4.1. Western Block, Kievev Deposit

Rock-forming minerals (clino- and orthopyroxenes, plagioclase) and the whole rock were analyzed in the gabbronorite SN-1 sampled from an olivine horizon of the Western Pansky block (Figure 5, Table 1). A Sm-Nd age of 2495 ± 24 Ma was obtained for these gabbronorites, the neodymium isotope composition corresponds to the $\epsilon_{Nd}(T)$ value of -2.4 . An age of 2498 ± 39 Ma was obtained for the gabbronorites SN-3 from the gabbronorite area of the intrusive. Yet, the neodymium isotope composition for these gabbronorites was less radiogenic, $\epsilon_{Nd}(T) = -0.3$, which can be related to isotope heterogeneity of differentiates.

A sample of the ore-hosting norite SN-6 containing Cu-Ni and Pt-Pd mineralization was taken from a lower contact of the Western Pansky block. Monomineralic fractions of ortho- and clinopyroxenes, plagioclase were isolated for studies. The Sm-Nd isochron of the isolated minerals and the whole rock corresponds to the age of 2484 ± 46 Ma (Figure 5, Table 1) with $\epsilon_{Nd}(T) = -0.2$.

Clino- and orthopyroxene, plagioclase, and a mixture of pyroxenes were isolated from the LLH ore gabbronorite sample, H-08-01. In the Sm-Nd diagram, these minerals and the whole rock (WR) form an isochron corresponding to the age of 2472 ± 33 Ma, where $\epsilon_{Nd}(T) = -2.9$. The Sm-Nd isotope age of the mineralized gabbro H-08-02 is 2470 ± 39 Ma (Figure 5, Table 1). The Sm-Nd ages obtained are similar to the U-Pb ages of LLH gabbro-

pegmatites, for which the age of 2470 ± 9 Ma was obtained [24]. The U-Pb age obtained for the sample H-08-01 is 2505 ± 5 Ma, and 2496 ± 8 Ma for the sample H-08-02 [55]. Such difference in the ages obtained using two separate methods can be explained by different temperatures of the closure of isotope systems in zircons and rock-forming minerals [56–58], as well as by the duration of rock cooling processes.

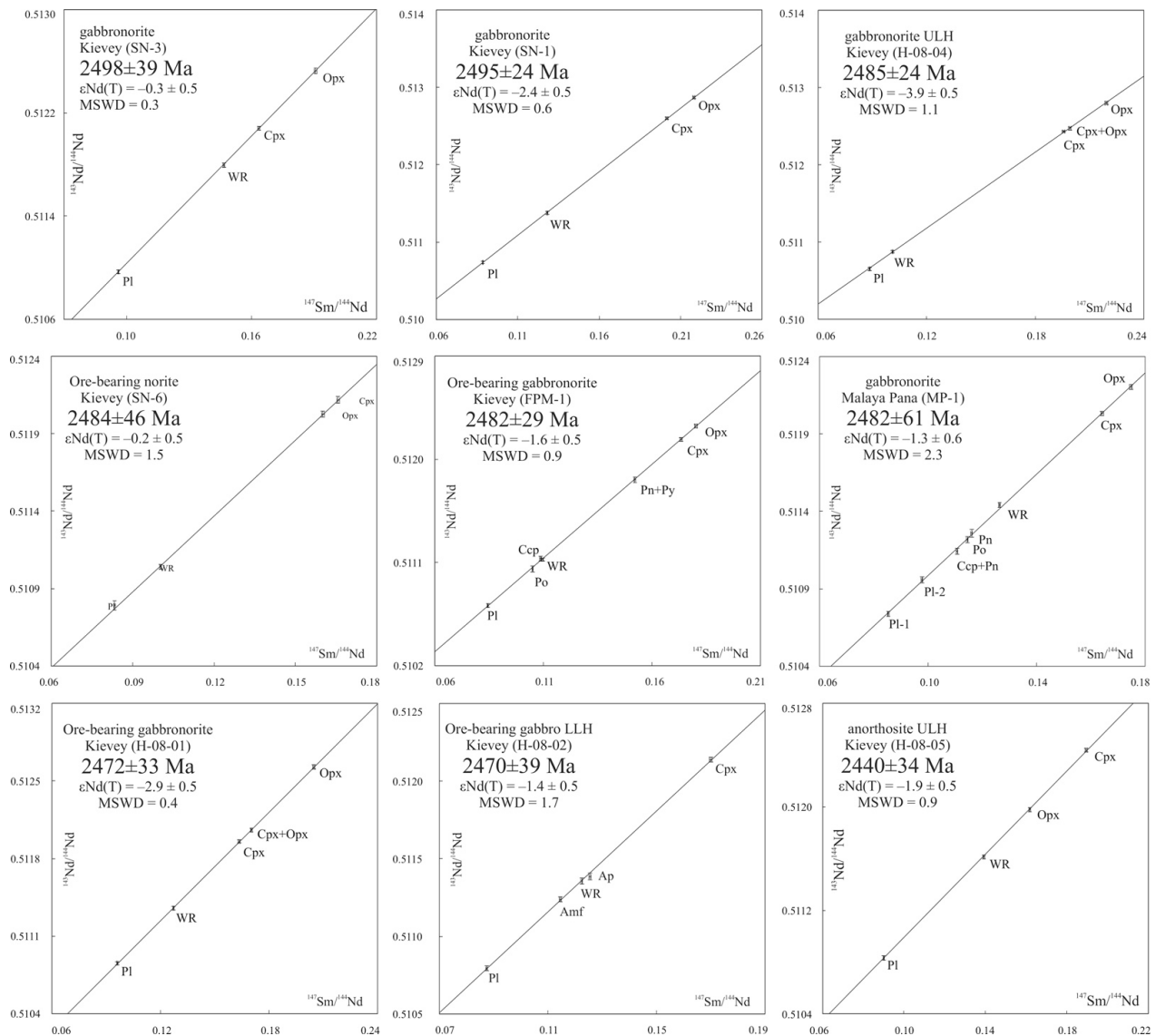


Figure 5. Mineral Sm-Nd isochrones for rocks of the Western Pansky block (Kievev deposit).

Clino- and orthopyroxene, plagioclase, and a mixture of pyroxenes were isolated from the ULH gabbronorites sample H-08-04. The Sm-Nd mineral isochron of these minerals and the whole rock combined gives the age of 2485 ± 24 Ma, where $\epsilon_{Nd}(T) = -0.4 \pm 0.5$ (Figure 5, Table 1). The age is interpreted as the age of crystallization of the upper-layered horizon gabbronorites. Particularly noteworthy is the anorthosite sample H-08-05. These anorthosites host the industrial Pt-Pd mineralization of the upper-layered horizon. Rock-forming minerals, i.e., plagioclase and clinopyroxene, were isolated from sample H-08-05 for Sm-Nd studies. In conjunction with the whole rock, they form a Sm-Nd mineral isochron with the age of 2442 ± 74 Ma (Figure 5, Table 1). From the literature, the U-Pb age (in baddeleyite) of these anorthosites is 2447 ± 12 Ma [24]. Yet, recent analyses based on studies of a drill sample of boreholes from the main anorthosite layer (MAL) and the U-Pb study of zircons using the SHRIMP-II allowed determining an older age for the ULH

anorthosites, i.e., 2509.4 ± 6.2 Ma [46]. Nowadays, the age of the upper-layered horizon anorthosites (or the main anorthosite layer) remains contentious and requires further study.

Clear monomineralic fractions of pyrrhotite, pentlandite, and a mixture of chalcopyrite with pentlandite, as well as rock-forming plagioclases and pyroxenes, of the LLH gabbro sample from the Kievev deposit (sample MP-1) were studied. The Sm-Nd isochron constructed for these minerals and the whole rock corresponds to the age of 2482 ± 61 Ma (Figure 5, Table 1). The $\epsilon\text{Nd(T)}$ parameter has a small negative value of -1.3 typical of Paleoproterozoic intrusions of the Baltic Shield. It indicates a mantle source with anomalous characteristics. Monomineralic fractions of rock-forming plagioclase and pyroxenes from ore gabbro sample (sample FPM-1) of the same stratiform deposit, as well as of ore pyrrhotite, chalcopyrite, and a mixture of pentlandite with pyrite, showed a Sm-Nd isochron age of 2482 ± 29 Ma (Figure 5, Table 1). The $\epsilon\text{Nd(T)}$ value of -1.6 also indicates an anomalous mantle source of magma, which formed the intrusive.

4.2. Fedorova Tundra

The Sm-Nd age of plagioclase, olivine, pyroxenes, and the whole rocks was obtained for harzburgite (F-1) from a lens-shaped body among gabbros of the taxite area. The age is 2494 ± 24 Ma, where $\epsilon\text{Nd(T)} = -1.0$. Within the limits of error, the obtained age is similar to the age of ore norite (F-2) containing the main industrial sulfide (Cu, Ni) and PGE (Pt, Pd, Rh) mineralization. The Sm-Nd isotope age of this norite is 2481 ± 24 Ma (Figure 6), and it indicates the formation time of ore differentiates of the Fedorova Tundra intrusive chamber of the layered complex. The rock has isotope characteristics of anomalous mantle, i.e., $\epsilon\text{Nd(T)} = -2.4$. The age obtained is interpreted as the age of ore mineralization formation within the Fedorova Tundra block of the intrusion.

Clino- and orthopyroxene, plagioclase, and the whole rock were studied in the orthopyroxenite sample (F-3). The age of 2523 ± 41 Ma (Figure 6) indicates the formation time of rocks of the most ancient ore-less intrusive, and is similar to the U-Pb age of zircon from the same sample, i.e., 2526 ± 6 Ma [26,55]. The $\epsilon\text{Nd(T)}$ value of -1.7 is typical of an anomalous mantle source [13]. The age obtained is the most ancient for the whole Paleoproterozoic Cu-Ni-PGE ore-magmatic system of the northeastern Baltic Shield.

A gabbro sample (F-4) was taken from a drill sample of the gabbro area of the Fedorova Tundra chamber of the intrusive. In the Sm-Nd diagram, cumulus plagioclase and orthopyroxene and intercumulus clinopyroxene, as well as the whole rock, give an isochron age of 2516 ± 23 Ma (Figure 6). The $^{147}\text{Sm}/^{143}\text{Nd}$ ratios for the studied rock vary from 0.08 to 0.22, which ensured obtaining a relatively small error for the age determination by the Sm-Nd method. The age thus obtained is similar to the U-Pb age of zircon 2516 ± 7 Ma [26,55]. The isotope composition of neodymium with $\epsilon\text{Nd(T)} = -1.4$ corresponds to an anomalous mantle source.

Orthopyroxene, plagioclase, clinopyroxene, and a mixture of clino- and orthopyroxene were isolated from the orthopyroxenite sample FT-1. In the Sm-Nd diagram, these minerals and the whole rock (WR) form an isochron of 2481 ± 32 Ma, where $\epsilon\text{Nd(T)} = -0.7$ (Figure 6). This age is interpreted as the age of orthopyroxenite intrusion onto the Fedorova Tundra block. The $\epsilon\text{Nd(T)}$ parameter of -0.7 indicates a mantle source of magmas with anomalous geochemical characteristics.

Pyroxenes (ortho- and clinopyroxene), plagioclase, and a mixture of sulfide minerals were also isolated from the gabbro sample FT-2. In conjunction with the whole rock, they form a Sm-Nd isochron with the age of 2491 ± 28 Ma, where $\epsilon\text{Nd(T)} = +1.0$ (Figure 6). The obtained age coincides with the earlier determined U-Pb age of zircons, which is 2491 ± 5 Ma [59]. This age indicates the time of crystallization of the Fedorova Tundra gabbros. The positive $\epsilon\text{Nd(T)}$ value atypical of rocks of layered intrusions can indicate a geochemically heterogeneous source of magmas, which formed the intrusive, or additional intruding injections of magmas with different isotope characteristics.

Orthopyroxene, plagioclase, and olivine were isolated from the olivine gabbro sample FT-3. The Sm-Nd mineral isochron for these minerals and the whole rock shows

an age of 2497 ± 32 Ma, where $\epsilon\text{Nd}(T) = -0.6$ (Figure 6). The obtained age indicates the formation time of the Fedorova Tundra gabbronorites. Compared to the U-Pb age of zircons [59], which is 2507 ± 11 Ma, a value of the Sm-Nd age is relatively younger, which can be related to different temperatures of the closure of isotope systems in zircons and rock-forming minerals. Yet, taking into account the age determination error in the Sm-Nd systematics, the obtained values are similar. The approximate age was obtained for the ore gabbro BGF-616, within which two generations of plagioclase, pyrite, chalcopyrite, and a mixture of pyrrhotite with pyrite were studied. In conjunction with the whole rock, they give the isochron age of 2493 ± 54 Ma (Figure 6), which indicates the time of formation of gabbro with sulfide mineralization.

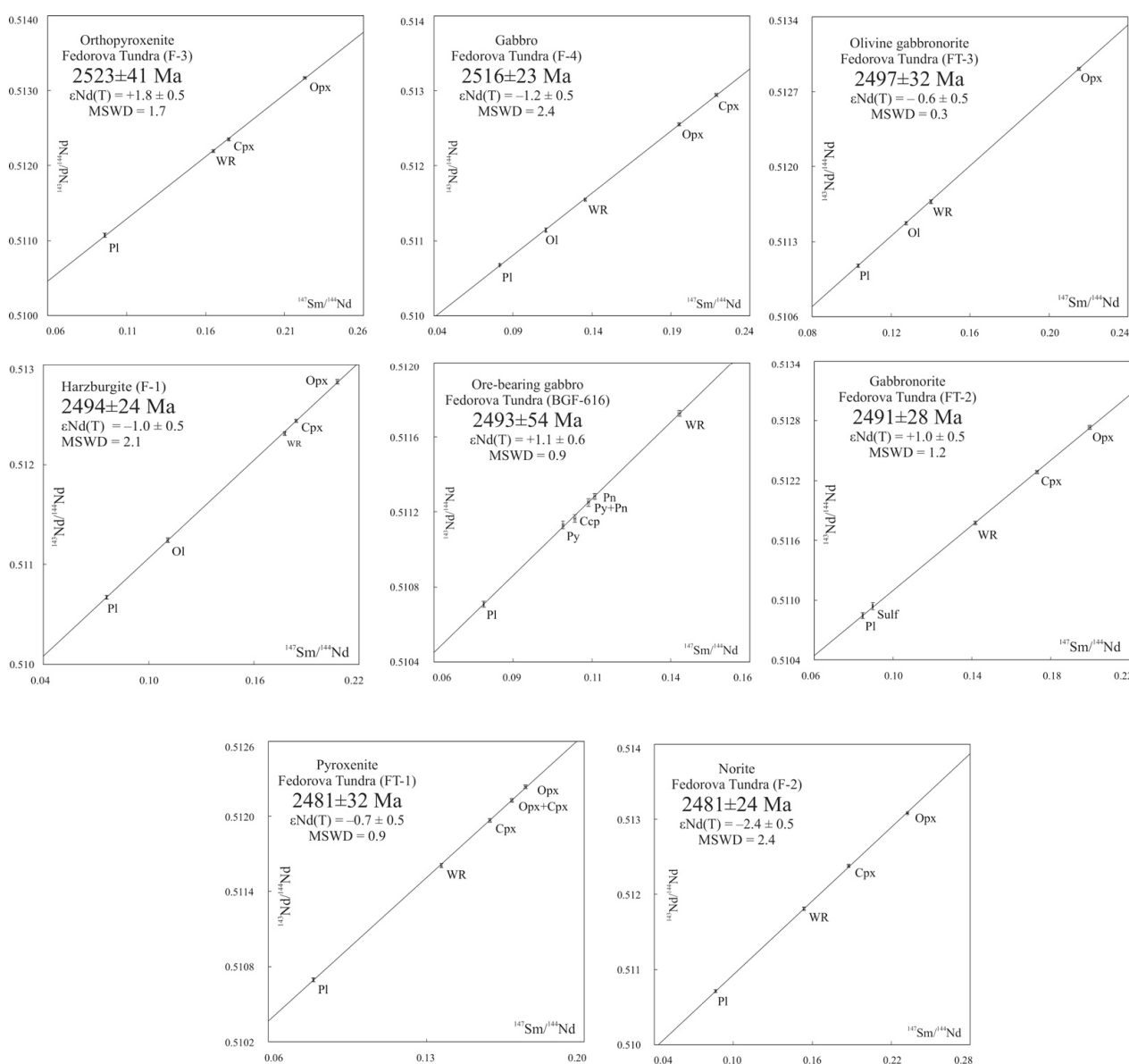


Figure 6. Mineral Sm-Nd isochrones for rocks of the Fedorova Tundra deposit.

4.3. Metamorphic Hydrothermal Events (Western Pansky Deposits)

The initial Sm-Nd isotope data from the minerals of metamorphic and hydrothermal origin (apatite, zoisite) for the gabbronorites of the North Kamennik deposit indicate the age of metamorphic transformations of 1.96–1.95 Ga (Figure 7). Noteworthy, these values

are close to the Sm-Nd age of the ore olivine norites from the Nyud-II (the Monchepluton, see below) of 1940 ± 32 Ma and to the age of epigenetic re-deposited ores of the Ahmavaara deposit of 1903 ± 24 Ma [31]. Close negative values of the $\epsilon_{Nd}(T)$ parameter from -5.6 to -7.2 may be connected with transformation of either regional metamorphic or hydrothermal metasomatic character due to the Svecofennian events.

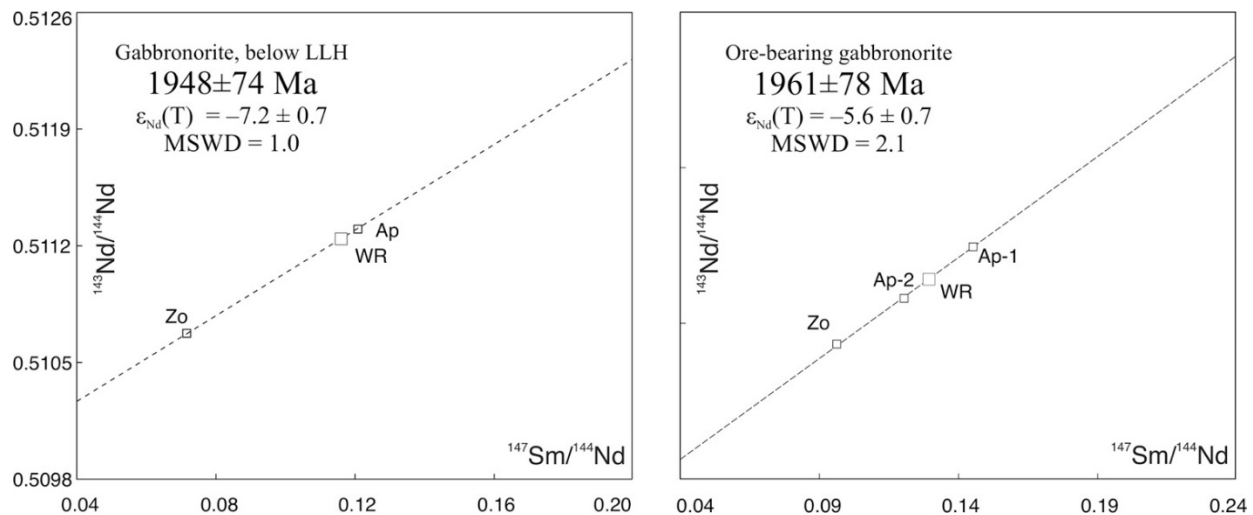


Figure 7. Metamorphic hydrothermal mineral Sm-Nd isochrones for gabbronorites of the North Kamennik deposit.

Analysis of Sm-Nd model ages for the Fedorova Tundra and Western Pansky blocks indicated that the age range of the Fedorova Tundra intrusive chamber is shifted to more ancient ages: model ages of the Western Pansky block vary within 2.8–3.1 Ga; the rocks of the Fedorova Tundra block have Sm-Nd model ages in the range of 2.9–3.4 Ga. This supports the hypothesis proposed earlier based on geological and isotope studies [24,41,55,59] that blocks of the complex formed from individual ore-magmatic chambers.

In general, the obtained Sm-Nd and U-Pb geochronological data are well intercorrelated, supplement each other, and allow getting reliable results during the dating of the composite layered complex. Such approach using separate and different isotope systems was successfully implemented not only during the study of the Fedorovo-Pansky complex, but also for other economic deposits of the Kola region [13,16,34,35].

The combined geological, mineralogical, and isotope-geochronological data allow defining at least three ore-magmatic systems within the Fedorovo-Pansky ore district: (1) troctolite-gabbronorite (2526–2507 Ma) with sulfide-intermetallic and arsenide mineral association of minerals of platinum metals (MPM); (2) norite-gabbronorite-anorthosite (2502–2470 Ma) with a prevalent sulfide-bismuth-telluride mineral association of MPM; (3) anorthosite (about 2.45 Ga) with low-temperature bismuth-telluride-sulfide mineral association of MPM. The first ore-magmatic system includes occurrences of ridges of the Fedorova Tundra massif; the second one includes the Fedorova Tundra, Kievev, and North Kamennik deposits; and the third one includes occurrences in the South Ridge of the Western Pansky massif. Therefore, the studies conducted indicate that the main industrial PGE mineralization of the Fedorovo-Pansky ore district is related to the norite-gabbronorite-anorthosite ore-magmatic system with the age of 2502–2470 Ma [60].

Therefore, the geochemical data allowed defining some special features of formation of the Fedorovo-Pansky layered complex. It was found that the Fedorova Tundra block was formed earlier than other structural blocks of the intrusive, which is supported by geochronological [56] and geological observations [60]. Older Sm-Nd model ages of rocks of this block, presence of taxite gabbronorites of the marginal area and diorite xenoliths (enclosing rocks), which are absent in other blocks of the intrusive [59], also indicate an early formation of the Fedorova Tundra intrusive chamber.

Complex isotope studies [24,46,55,59] allowed finding reliable age constraints of the platiniferous Fedorovo-Pansky massif formation:

- 2526–2516 Ma—early pyroxenites and gabbro of the Fedorova Tundra deposit;
- 2502–2485 Ma—gabbro and gabbro of the ore-magmatic chambers of the Western Pansky block, earlier disseminated PGE mineralization and enriched Cu-Ni sulfide mineralization in marginal parts of the intrusive (Fedorova Tundra deposit);
- 2470 Ma—pegmatoid gabbro-anorthosites with enriched PGE mineralization from the lower layered horizon;
- 2445–2440 Ma—late anorthosite injections and lens-shaped bodies of enriched Pt-Pd ore occurrences of the upper layered horizon.

4.4. Monchetundra Intrusion

The results of Sm-Nd isotope geochronological research are displayed in Table 2 and in Figures 8–10.

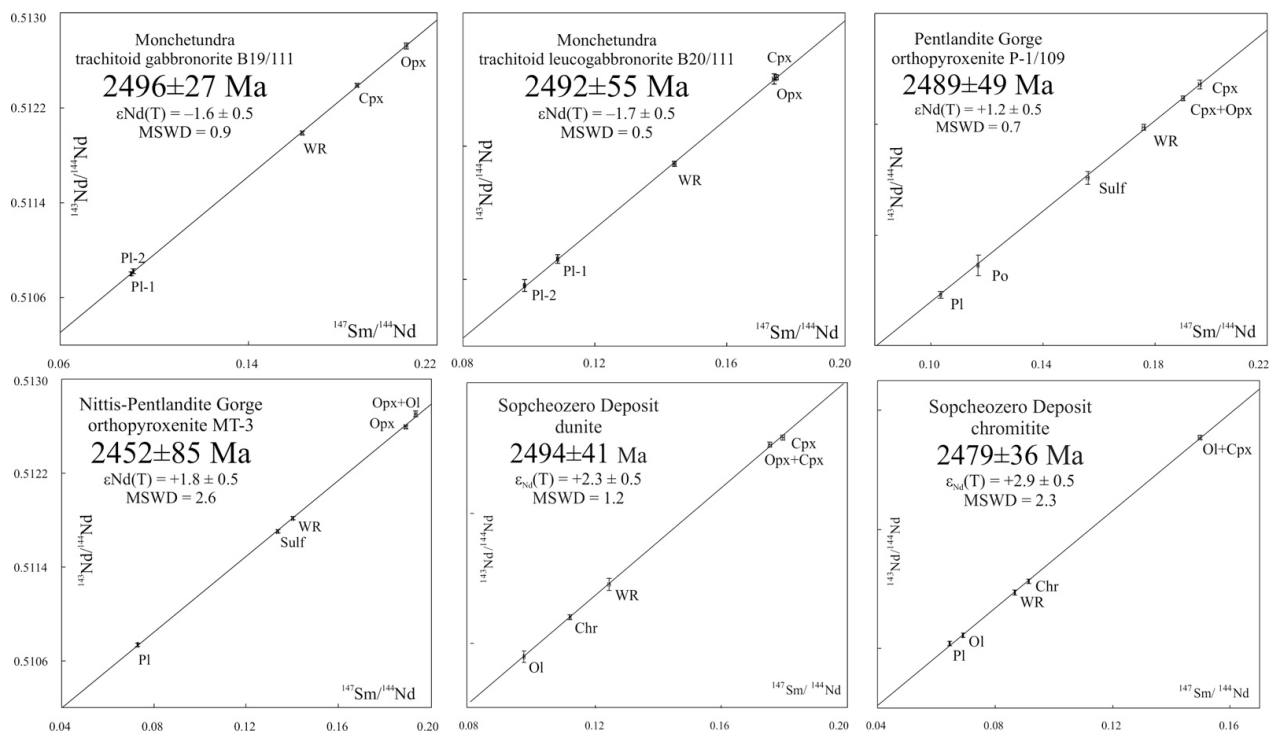


Figure 8. Mineral Sm-Nd isochrones for rocks of the Monchetundra area.

The Sm-Nd mineral isochron for orthopyroxene, olivine, plagioclase, sulfide minerals, and the whole rock (orthopyroxenites from lower zone of the Monchetundra massif, sample MT-3) determines the age of 2452 ± 85 Ma (Figure 8, Table 2). Positive value of $\epsilon_{Nd}(T) = +1.8$ shows the presence of low-depleted mantle source and may indicate the additional injections of magmas with unusually positive $\epsilon_{Nd}(T)$ isotope characteristics [3,4,34–37]. The age obtained is close to that of orthopyroxenites from the Pentlandite Valley (sample P-1/109) – 2489 ± 49 Ma, $\epsilon_{Nd}(T) = +1.2$ within the limits of error.

The Sm-Nd mineral isochrons for gabbro and leucogabbro (samples B19/111 and B20/111) indicate a similar age and common isotope characteristics of parental melt, i.e., 2496 ± 27 Ma and 2492 ± 55 Ma respectively (Figure 8, Table 2). Values of $\epsilon_{Nd}(T) = -1.6 \pm 0.5$ and -1.7 ± 0.5 indicate the common source of magma that formed the intrusion.

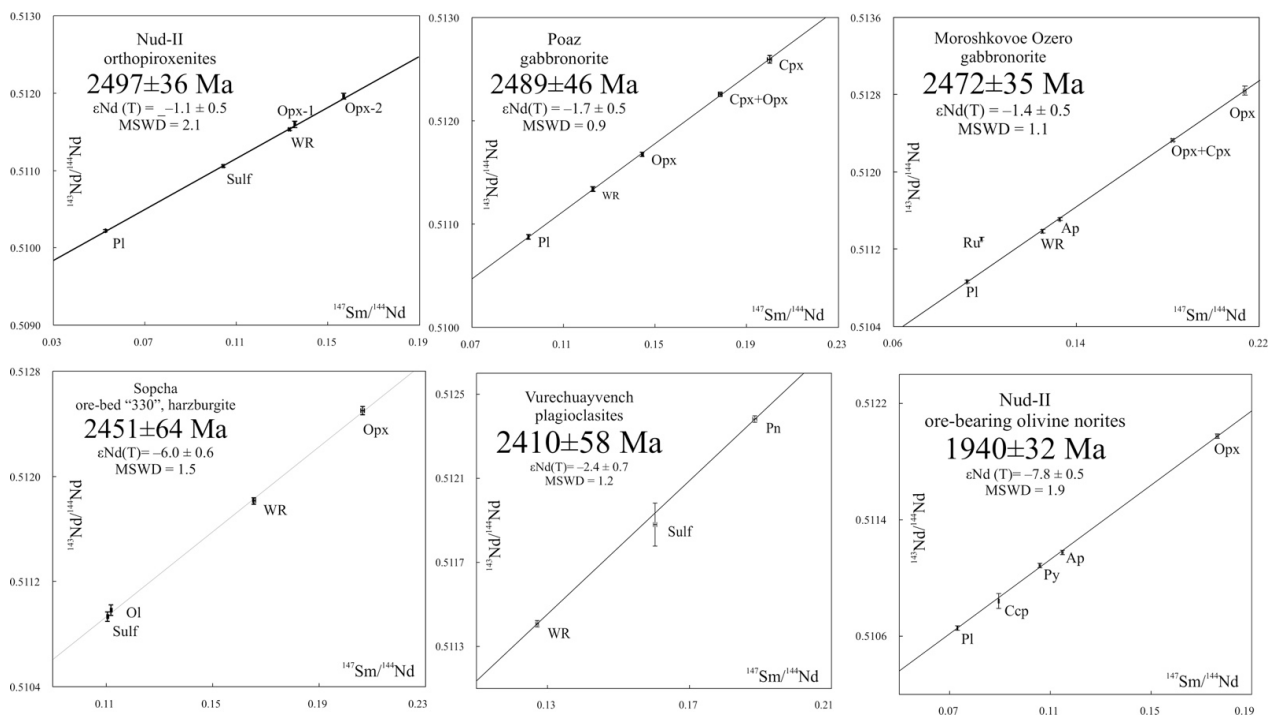


Figure 9. Mineral Sm-Nd isochrones for rocks of the Monchepluton complex.

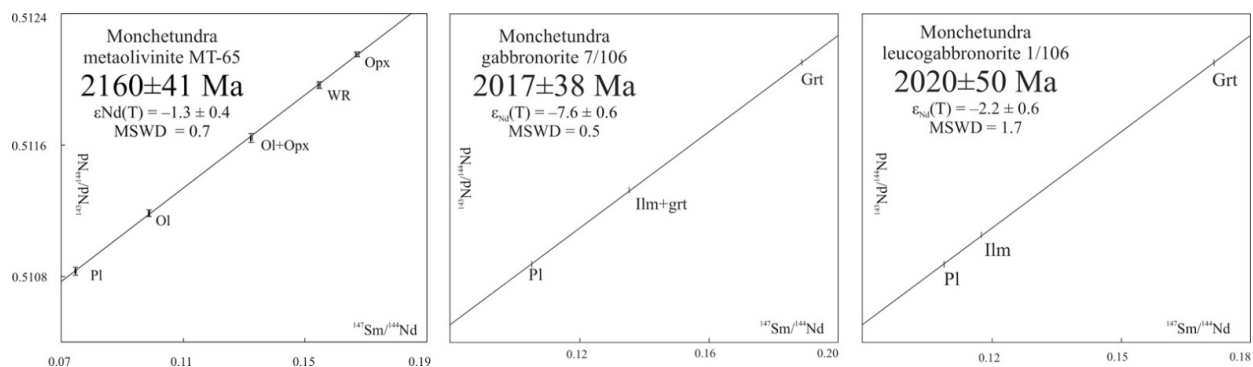


Figure 10. Mineral Sm-Nd isochrones for rocks of the Monchetundra massif.

Dunites and chromitite interlayers are dated in the Sopchezero deposit. The Sm-Nd mineral isochron for dunites (sample 404, Figure 8) indicates an age of 2494 ± 41 Ma, $\epsilon_{\text{Nd}}(T) = +2.3 \pm 0.5$. Meanwhile the distinctive features of chromitites from the Sopchezero deposit (sample 405, Figure 8) are their younger Sm-Nd age of 2479 ± 36 Ma and more radiogenic isotope composition of neodymium with $\epsilon_{\text{Nd}}(T) = +2.9 \pm 0.5$. This indicates later intrusion of the chromium-rich magmas in the aftermath of additional injection. Nevertheless, the origin of chromitite dykes of the Sopchezero deposit is still object of debate. There are several hypotheses regarding the matter: (a) an intrusion from an underlying magma chamber; (b) remobilization of chromites at the later formation stage and their intrusion into the hosting dunites; (c) chromite crystallization on the walls of a feeder [61]. The age data support later chromite formation. This however may possibly mean that the geochronological “watch” is slow, i.e., the chromite layer formation takes more time because of the prolonged crystallization. Yet, another possible way to generate the chromite layers is formation of chromium-rich melts that rise due to the lithostatic pressure fall [62]. This pioneering hypothesis needs further investigation, as it looks promising and well founded.

4.5. Monchepluton

The Sm-Nd isotope data obtained from sulfide minerals, olivine, and the whole rock indicate an age of 2497 ± 36 Ma for orthopyroxenites from the Nyud-II open pit (Figure 9). This value is close to the results of U-Pb analysis of zircon, i.e., 2503 ± 8 Ma [37,49]. Meanwhile, the analysis of ore olivine norites from the Nyud-II shows a far younger Sm-Nd age of 1940 ± 32 Ma (Figure 9), and the U-Pb analysis of zircons from this sample gives a value of 2506 ± 3 Ma [37]. Such data may most likely be interpreted as follows: hydrothermal metasomatic processes led to the disturbance of the Sm-Nd isotope systems of minerals in the course of formation of ore mineralization. In this case, the obtained age corresponds to the age of the last disturbance of the Sm-Nd isotope system.

The Sm-Nd results for the olivine orthopyroxenites from the Horizon 330 ore layer (Mt. Sopcha) are of great importance. The Sm-Nd mineral isochron for orthopyroxene, olivine, sulfide minerals, and the whole rock indicates an age of 2451 ± 64 Ma, where $\epsilon\text{Nd}(T) = -6.0 \pm 0.6$. These data are interpreted as the formation time of orthopyroxenites hosting the ore layer; the latter was formed as a result of pulsed refilling the Monchepluton Eastern magmatic chamber with a fresh batch of high-temperature non-differentiated high-magnesia melt [4,37,49]. Anomalously low value of $\epsilon\text{Nd}(T) = -6.0$ for these orthopyroxenites apparently depends on high contamination of parental magmas with the crustal matter [37,49].

The Sm-Nd mineral isochron for gabbro-norites from Mt. Poaz determines their age value of 2489 ± 46 Ma, where $\epsilon\text{Nd}(T) = -1.7$ (Figure 9). The gabbro-norites are stratigraphically in the upper parts of the complex (Figure 3). The ages obtained are close to data from the U-Pb analysis of plagioclases of the Vurechuayvench deposit (2494 ± 4 Ma [37]). The plagioclases are also positioned in the upper parts of the section, and they define the upper age limit of the Monchegorsk complex. However, Sm-Nd mineral age of these ore plagioclases from the Vurechuayvench deposit (Figure 9), i.e., 2410 ± 58 Ma differs from the U-Pb age. It may indicate a considerable influence of metamorphic and hydrothermal metasomatic transformations of massif on the process of platiniferous ore genesis. Yet these rejuvenated age data are similar to the U-Pb age of hydrothermal metasomatic transformations of anorthosites of the Volchetundra massif (2407 ± 3 Ma [63]) and metamorphism of the Monchetundra massif (2406 ± 3 Ma [28]). So the obtained Sm-Nd age of plagioclases from the Vurechuayvench deposit likely reflects sulfide ore genesis, taking into consideration that we used a mixture of sulfides and pentlandite to carry out the analysis. Noteworthy, the sulfide ore genesis processes may considerably deviate from the time of rock crystallization [37].

The Sm-Nd mineral isochron for gabbro-norites from the Moroshkovoe Lake (Figure 9) indicates the age of 2472 ± 35 Ma, where $\epsilon\text{Nd}(T) = -1.4 \pm 0.5$, matching the U-Pb age for zircon (2463.1 ± 2.7 Ma [37]) within the limits of error. The obtained geochronological data show that rocks of the Moroshkovoe Lake massif were formed during the late stages of magmatism in the Monchegorsk ore district. More specifically, these age data appear to be close to that of the Volchetundra gabbro-anorthosites massif rocks, i.e., 2473 ± 7 and 2463 ± 2.4 Ma for leuconorites from the marginal zone and 2467 ± 8 Ma for leucogabbro from the main zone [63].

4.6. Metamorphic Events (Monchetundra Intrusion)

The rejuvenated Sm-Nd age value of 2160 ± 41 Ma (Figure 10) was obtained for the metaolivinites from the Loipishnyun unit (MT-65). The rock is strongly metamorphosed; it contains relics of olivine and plagioclase. The pyroxenes are almost entirely replaced by serpentine. The age values obtained correspond to the time of late metamorphic transformation of the Monchetundra massif rocks and are close to the age of leucogabbro-norites (2020 ± 50 Ma) and gabbro-norite-anorthosites of the Loipishnyun unit [64] within the limits of error. A geochronological stage ca. 2.0 Ga marks the time of foundation and development of the Monchegorsk fault. This fault divides the Monchegorsk pluton and the Main Ridge massif, being a part of the regional Central Kola fault system. The research of

metamorphic minerals from blastomylonites uncovered by the record hole M-1 shows that the Monchetundra fault formation began ca. 2.0–1.9 Ga, together with the Svecofennian orogen [65].

Therefore, the history of the Monchegorsk complex formation lies within the 2.51–2.49 Ga range in accordance with the Sm-Nd and U-Pb geochronological data. Meanwhile the history of the Fedorovo-Pansky complex occupies a more prolonged range of 2.53–2.47 Ga. On the other hand, both the manifestation time of hydrothermal metasomatic processes and the injection of additional magma batches within these two complexes refer to the age of 2.47–2.44 Ga.

4.7. Magma Sources and Crustal Contamination

According to the geochronological and Nd-Sr isotope data [11–13], the rocks of the Monchegorsk and the Fedorovo-Pansky complexes seem to share a common mantle source with the Paleoproterozoic layered intrusions of the Fennoscandian Shield (Figure 11). The data obtained are consistent with the known isotope-geochemical and geochronological characteristics of ore-bearing layered intrusions in the northeastern Baltic Shield [13,24,34]. The rocks of these intrusions that belong to the pyroxenite-gabbro-norite-anorthosite formation had similar isotope-geochemical features [13,34]. Along with the intrusive complexes of Finland, these intrusions are linked with the Matachewan Large Igneous province of the southern Superior craton [66].

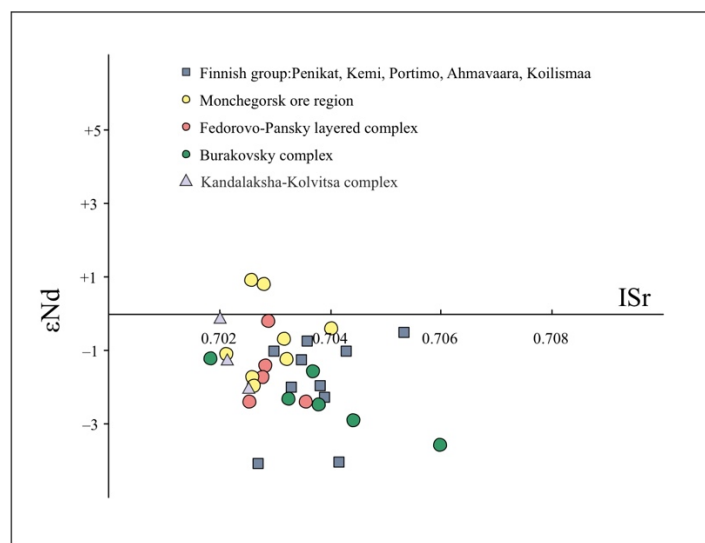


Figure 11. Variations of ϵNd vs. ISr in rocks of Paleoproterozoic layered intrusions in the Fennoscandian Shield. Data for Finnish group, Burakovsky and Kandalaksha-Kolvitsa complexes from [13,16,17,67].

Numerous publications concerning the issues of magma sources for the layered intrusions come to two main conclusions in the form of hypotheses. The first is that the intrusions could be formed directly from a mantle source bearing anomalous isotope characteristics: negative ϵNd values and low ISr 0.702–0.705. The other is that the negative values of $\epsilon\text{Nd(T)}$ parameter are associated with the crustal contamination processes.

To evaluate the contamination level we used the binary shift model [68]. It allowed us to determine the mantle component share in a mantle-crust mixture. For the Fedorovo-Pansky Complex, we used data for hosting diorites as a crustal end-member, i.e., $\epsilon\text{Nd} = -4.5$ and $\text{Nd} = 13.0$ ppm. For the Monchegorsk Complex we used tonalites of the Voche-Lambina as a crustal component with $\epsilon\text{Nd} = -3.5$ and $\text{Nd} = 30.0$ ppm [69]. Additional calculations were made to measure the crustal component share for the Olanga intrusion group (the Tsipringa, the Lukkulaisvaara, the Kivakka) and the Burakovsky complex (isotope data taken from [70]). For the Burakovskaya intrusion, we used crustal

component data from the Vodlozersky domain where $\epsilon\text{Nd} = -5.1$ and $\text{Nd} = 6.4$ ppm [71]. For the Olanga intrusion group, we used the crust parameters where $\epsilon\text{Nd} = -5.0$ and $\text{Nd} = 27.0$ ppm [72]. The obtained data (Figure 12) indicate a small degree of contamination (5–15% of the crustal component). However, the crustal component share of the Monchetundra complex rocks is considerably higher (up to 80%) in amphibolized gabbroids of the massif margins than in the central part rocks (about 10%). This indicates the high probability of active interaction of melt and crustal matter within the contact zones of massif and host rocks.

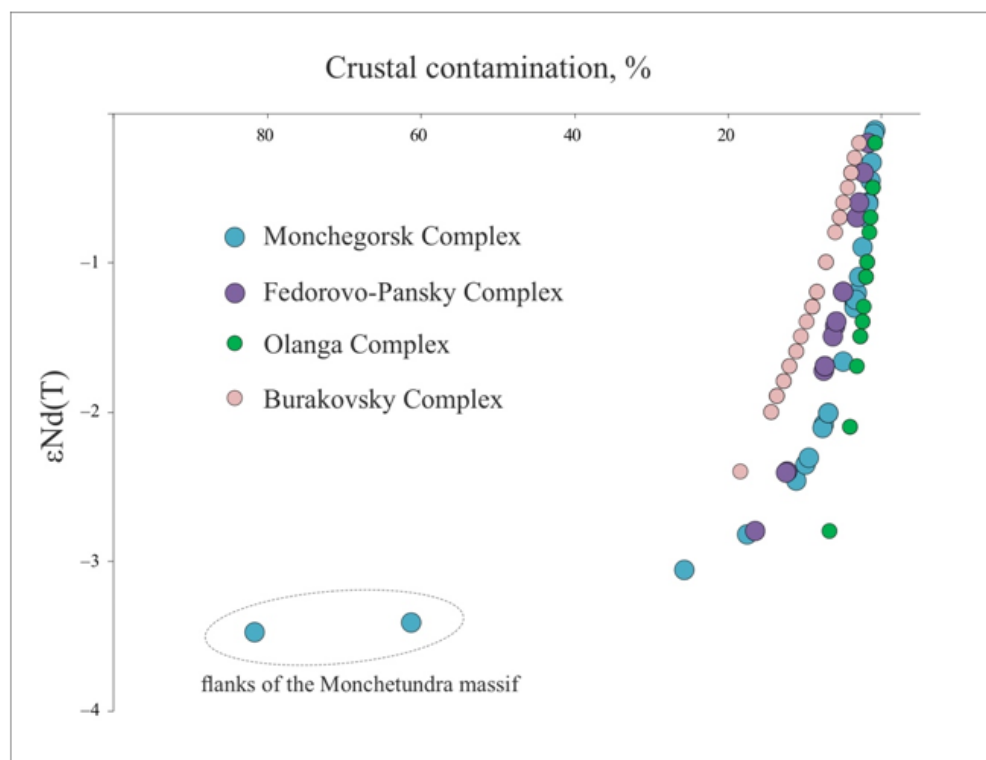


Figure 12. Contribution of the crustal component (crustal contamination) in the rocks of the layered intrusions of the Fennoscandian Shield. Data for the Burakovsky intrusion and the Olanga group from [70].

5. Conclusions

1. We obtained reliable data regarding the age and isotope characteristics of the two largest ore complexes of the northeastern Baltic Shield, i.e., the Cu-Ni-Cr Monchegorsk complex and the Pt-Pd Fedorovo-Pansky complex.
2. Injection of additional magma batches within the studied complexes occurred at an age of 2.45 Ga. The age of platiniferous reef harzburgites of the Sopcha Horizon 330 (2451 ± 64 Ma) and close Sm-Nd age of the ULH anorthosites of the Western Pansky massif (2447 ± 34 Ma) are consistent with their formation, i.e., the injection of additional batches of crust-contaminated magma.
3. Rejuvenated Sm-Nd age values are obtained for the PGE-bearing plagioclases from the Vurechuayvench deposit and norites from the Nyud-II deposit. The values indicate a considerable influence of hydrothermal metasomatic transformations on the platiniferous ore genesis. Close age values are also obtained for the PGE-bearing gabbro-norites and gabbro from the Western Pansky massif, i.e., 2473 ± 30 Ma and 2470 ± 39 Ma, respectively.
4. Ore genesis of the layered complexes is greatly influenced by the injections of additional magma batches and the hydrothermal metasomatic transformations. The defined formation stages of the largest Paleoproterozoic layered complexes in the

northeastern Baltic Shield are also found elsewhere including the Canadian Shield. The metamorphic transformations leading to the formation of redeposited ores at the age of 2.0–1.9 Ga coincided with the beginning of the Svecofennian events, widely presented on the Fennoscandian shield.

5. The interaction model of parental melt of layered intrusions and crustal matter indicates a small contamination level. However, the crustal contamination increases considerably on the margins of the Monchetundra massif because of the active interaction of parental magmas and host rock.

Funding: This research was funded by the Ministry of Science and Higher Education of the Russian Federation (project 0226-2019-0053).

Institutional Review Board Statement: Not applicable.

Informed Consent Statement: Not applicable.

Data Availability Statement: Not applicable.

Acknowledgments: The studies are dedicated to the memory of the RAS academician F.P. Mitrofanov, under whose guidance a major part of the presented results was obtained. The author expresses his appreciation to T.B. Bayanova, Head of Laboratory of Geochronology and Isotope Geochemistry (Geological Institute of the Kola Science Centre, Russian Academy of Sciences), for general guidance on the studies and assistance during their implementation. The author thanks O.G. Sherstenikova and N.A. Ekimova (Geological Institute of the Kola Science Centre) for their help in the chemical preparation of the rocks; L.I. Koval (Geological Institute of the Kola Science Centre) for extraction of the mineral fractions and grinding of the rocks. The author is also grateful to V.V. Chaschin, E.L. Kunakkuzin, E.N. Steshenko, E.S. Borisenko, and L.I. Nerovich for their help and advice during the field investigation, preliminary sample preparation, and analytical research.

Conflicts of Interest: The author declares no conflict of interest.

References

1. Karykowski, B.T.; Maier, W.D.; Groshev, N.Y.; Barnes, S.-J.; Pripachkin, P.V.; McDonald, I.; Savard, D. Critical controls on the formation of contact-style PGE-Ni-Cu mineralization: Evidence from the Paleoproterozoic Monchegorsk Complex, Kola region, Russia. *Econ. Geol.* **2018**, *113*, 911–935. [[CrossRef](#)]
2. Maier, W.D.; Hanski, E.J. Layered mafic-ultramafic intrusions of Fennoscandia: Europe's treasure chest of magmatic metal deposits. *Elements* **2017**, *13*, 415–420. [[CrossRef](#)]
3. Nerovich, L.I.; Bayanova, T.B.; Serov, P.A.; Elizarov, D.V. Magmatic sources of dikes and veins in the Moncha Tundra Massif, Baltic Shield: Isotopic-geochronologic and geochemical evidence. *Geochem. Int.* **2014**, *52*, 548–566. [[CrossRef](#)]
4. Sharkov, E.V.; Chistyakov, A.V. Geological and petrological aspects of Ni-Cu-PGE mineralization in the Early Paleoproterozoic Monchegorsk layered mafic-ultramafic complex, Kola Peninsula. *Geol. Ore Depos.* **2014**, *56*, 147–168. [[CrossRef](#)]
5. Yang, S.H.; Hanski, E.; Li, C.; Maier, W.D.; Huhma, H.; Mokrushin, A.V.; Latypov, R.; Lahaye, Y.; O'Brien, H.; Qu, W.-J. Mantle source of the 2.44–2.50-Ga mantle plume-related magmatism in the Fennoscandian Shield: Evidence from Os, Nd and Sr isotope compositions of the Monchepluton and Kemi intrusions. *Miner. Depos.* **2016**, *51*, 1055–1073. [[CrossRef](#)]
6. Hanski, E.; Huhma, H.; Smolkin, V.F.; Vaasjoki, M. The age of the ferropicritic volcanics and comagmatic Ni-bearing intrusions at Pechenga, Kola Peninsula, USSR. *Bull. Geol. Soc. Finl.* **1990**, *62*, 123–133. [[CrossRef](#)]
7. Sharkov, E.V.; Smolkin, V.F. The Early Proterozoic Pechenga-Varzuga Belt: A case history of Precambrian back-arc spreading. *Precambrian Res.* **1997**, *82*, 133–151. [[CrossRef](#)]
8. Walker, R.J.; Morgan, J.W.; Hanski, E.J.; Smolkin, V.F. Re-Os systematics of early Proterozoic ferropicrites, Pechenga complex, NW Russia: Evidence for ancient ¹⁸⁷Os-enriched plumes. *Geochim. Cosmochim. Acta* **1997**, *61*, 3145–3160. [[CrossRef](#)]
9. Neradovsky, Y.N.; Alekseeva, S.A.; Chernousenko, E.V. Mineralogy and process properties of Kolvitsky titanomagnetite ore. *IOP Conf. Ser. Earth Environ. Sci.* **2019**, *262*, 012050. [[CrossRef](#)]
10. Voitekhovskii, Y.L.; Neradovskii, Y.N.; Grishin, N.N.; Rakitina, E.Y.; Kasikov, A.G. The Kolvitskoe deposit (geology, material composition of ores). *Vestn. MGTU* **2014**, *17*, 271–278.
11. Serov, P.A. Pt-bearing Fedorovo-Pansky Layered Complex (Kola Peninsula): Sm-Nd geochronology and Nd-Sr characteristics. *IOP Conf. Ser. Earth Environ. Sci.* **2020**, *539*, 012166. [[CrossRef](#)]
12. Baynova, T.; Ludden, J.; Mitrovanov, F. Timing and duration of Paleoproterozoic ore-bearing layered intrusions of the Baltic Shield: Metallogenic, petrological and geodynamic implications. In *Paleoproterozoic Supercontinents and Global Evolution*; Reddy, S.M., Mazumder, R., Evans, D.A., Collins, A.S., Eds.; Geological Society of London: London, UK, 2009; Volume 323, pp. 165–198.

13. Mitrofanov, F.P.; Bayanova, T.B.; Ludden, J.N.; Korchagin, A.U.; Chashchin, V.V.; Nerovich, L.I.; Serov, P.A.; Mitrofanov, A.F.; Zhironov, D.V. Origin and Exploration of the Kola PGE-bearing Province: New Constraints from Geochronology. In *Ore Deposits: Origin, Exploration, and Exploitation*; Geophysical Monograph Series; Sophie Decree, S., Robb, L., Eds.; Wiley: Hoboken, NJ, USA, 2019; pp. 3–36.
14. Mitrofanov, F.; Golubev, A. Russian Fennoscandian metallogeny. In *Abstracts of the 33 IGC*; Norwegian Academy of Science and Letters: Oslo, Norway, 2008.
15. Schissel, D.; Tsvetkov, A.A.; Mitrofanov, F.P.; Korchagin, A.U. Basal Platinum-Group Element Mineralization in the Fedorov Pansky Layered Mafic Intrusion, Kola Peninsula, Russia. *Econ. Geol.* **2002**, *97*, 1657–1677. [[CrossRef](#)]
16. Amelin, Y.V.; Heaman, L.M.; Semenov, V.S. U-Pb geochronology of layered mafic intrusions in the eastern Baltic Shield: Implications for the timing and duration of Paleoproterozoic continental rifting. *Precambrian Res.* **1995**, *75*, 31–46. [[CrossRef](#)]
17. Huhma, H.; Clift, R.A.; Perttunen, V.; Sakko, M. Sm-Nd and Pb isotopic study of mafic rocks associated with early Proterozoic continental rifting: The Perapohja schist belt in northern Finland. *Contrib. Mineral. Petrol.* **1990**, *104*, 369–379. [[CrossRef](#)]
18. Halkoaho, T.; Alapieti, T.T.; Lahtinen, J.J. The Sompujarvi PGE mineralization in the Penikat layered intrusion. In *Proceedings of the 5th International Platinum Symposium: Guide to the Post-Symposium Field Trip*, Helsinki, Finland, 4–11 August 1989; Volume 29, pp. 71–92.
19. Halkoaho, T.A.A.; Alapieti, T.T.; Lahtinen, J.J. The Sompujarvi PGE Reef in the Penikat layered intrusion, Northern Finland. *Miner. Pet.* **1990**, *42*, 39–55. [[CrossRef](#)]
20. Hanski, E.; Walker, R.J.; Huhma, H.; Suominen, I. The Os and Nd isotopic systematics of c. 2.44 Ga Akanvaara and Koitelainen mafic layered intrusions in northern Finland. *Precambrian Res.* **2001**, *109*, 73–102. [[CrossRef](#)]
21. Iljina, M.; Maier, W.D.; Karinen, T. PGE-(Cu-Ni) deposits of the Tornio-Näränkäväära belt of intrusions (Portimo, Penikat and Koillismaa). In *Mineral Deposits of Finland*; Maier, W.D., Lahtinen, R., O'Brien, H., Eds.; Elsevier: Amsterdam, The Netherlands, 2015; pp. 133–164.
22. Smith, W.D.; Maier, W.D. The geotectonic setting, age and mineral deposit inventory of global layered intrusions. *Earth-Sci. Rev.* **2021**, *220*, 103736. [[CrossRef](#)]
23. Balashov, Y.A.; Bayanova, T.B.; Mitrofanov, F.P. Isotope data on the age and genesis of layered basic-ultrabasic intrusions in the Kola Peninsula and northern Karelia, northeastern Baltic Shield. *Precambrian Res.* **1993**, *64*, 197–205. [[CrossRef](#)]
24. Bayanova, T.B. *Age of Reference Geological Complexes of the Kola Region and the Duration of Igneous Processes*; Nauka: Saint Petersburg, Russia, 2004; p. 174. (In Russian)
25. Bayanova, T.B. Baddeleyite: A promising geochronometer for alkaline and basic magmatism. *Petrology* **2006**, *14*, 187–200. [[CrossRef](#)]
26. Serov, P.A.; Nitkina, E.A.; Bayanova, T.B.; Mitrofanov, F.P. Comparison of new U-Pb and Sm-Nd isotope data on rocks of the early barren phase and basal ore-bearing rocks in the PGE-bearing Fedorovo-Pana layered massif, Kola Peninsula. *Dokl. Earth Sci.* **2007**, *416*, 1125–1127. [[CrossRef](#)]
27. Huhma, H.; Mutanen, N.; Hanski, E. Sm-Nd isotopic evidence for contrasting sources of the prolonged Paleoproterozoic mafic-ultramafic magmatism in Central Finnish Lapland. In *Proceedings of the IGCP Project 336 Symposium*, Rovaniemi, Finland, 21–23 August 1996; Volume 33, pp. 57–58.
28. Mitrofanov, F.P.; Balagansky, V.V.; Balashov, Y.A.; Gannibal, L.F.; Dokuchaeva, V.S.; Nerovich, L.I.; Radchenko, M.K.; Ryungenen, G.I. U-Pb age for gabbro-anorthosite of the Kola Peninsula. *Dokl. Earth Sci.* **1993**, *331*, 95–98.
29. Peltonen, P.; Brugmann, G. Origin of layered continental mantle (Karelian craton, Finland): Geochemical and Re-Os isotope constraints. *Lithos* **2006**, *89*, 405–423. [[CrossRef](#)]
30. Puchtel, I.S.; Brugmann, G.E.; Hofmann, A.W.; Kulikov, V.S.; Kulikova, V.V. Os isotope systematics of komatiitic basalts from the Vetreny belt, Baltic Shield: Evidence for a chondritic source of the 2.45 Ga plume. *Contrib. Mineral. Petrol.* **2001**, *140*, 588–599. [[CrossRef](#)]
31. Serov, P.A.; Ekimova, N.A.; Bayanova, T.B.; Mitrofanov, F.P. Sulfide minerals as new geochronometers during Sm-Nd dating of the ore genesis for layered mafic and ultramafic intrusions. *Lithosphere* **2014**, *4*, 11–21.
32. Sharkov, E.V. *Petrology of Layered Intrusions*; Nauka: Saint Petersburg, Russia, 1980; p. 183. (In Russian)
33. Vogel, D.C.; Vuollo, J.I.; Alapieti, T.T.; James, R.S. Tectonic, stratigraphic and geochemical comparison between ca. 2500–2440 Ma mafic igneous events in the Canadian and Fennoscandian Shields. *Precambrian Res.* **1998**, *92*, 89–116. [[CrossRef](#)]
34. Bayanova, T.; Korchagin, A.; Mitrofanov, A.; Serov, P.; Ekimova, N.; Nitkina, E.; Kamensky, I.; Elizarov, D.; Huber, M. Long-lived mantle plume and polyphase evolution of Palaeoproterozoic PGE intrusions in the Fennoscandian Shield. *Minerals* **2019**, *9*, 59. [[CrossRef](#)]
35. Bayanova, T.; Mitrofanov, F.; Serov, P.; Nerovich, L.; Yekimova, N.; Nitkina, E.; Kamensky, I. Layered PGE Paleoproterozoic (LIP) Intrusions in the N-E Part of the Fennoscandian Shield—Isotope Nd-Sr and ³He/⁴He Data, Summarizing U-Pb Ages (on Baddeleyite and Zircon), Sm-Nd Data (on Rock-Forming and Sulphide Minerals), Duration and Mineralization. In *Geochronology—Methods and Case Studies*; Morner, N.-A., Ed.; Intech: London, UK, 2014; pp. 143–193.
36. Bayanova, T.B.; Rundkvist, T.V.; Serov, P.A.; Korchagin, A.U.; Karpov, S.M. The Palaeoproterozoic Fedorovo-Pansky layered PGE Complex of the northeastern Baltic Shield, Arctic Region: New U-Pb (Baddeleyite) and Sm-Nd (Sulfide) data. *Dokl. Earth Sci.* **2017**, *472*, 1–5. [[CrossRef](#)]

37. Chashchin, V.V.; Bayanova, T.B.; Mitrofanov, F.P.; Serov, P.A. Low-sulfide PGE ores in Palaeoproterozoic Monchegorsk Pluton and massifs of its southern framing, Kola Peninsula, Russia: Geological characteristic and isotope geochronological evidence of polychronous ore-magmatic systems. *Geol. Ore Depos.* **2016**, *58*, 37–57. [[CrossRef](#)]
38. Ernst, R.E. *Large Igneous Provinces*; Cambridge University Press: Cambridge, UK, 2014; p. 653.
39. Alapieti, T.; Filen, B.; Lahtinen, J.; Lavrov, M.; Smolkin, V.; Voitsekhovskiy, S. Early Proterozoic layered intrusions in the northeastern part of the Fennoscandian Shield. *Miner. Pet.* **1990**, *42*, 1–22. [[CrossRef](#)]
40. Melezhik, V.A.; Hanski, E.J. The Pechenga Greenstone Belt. In *Reading the Archive of Earth's Oxygenation, Volume 1: The Palaeoproterozoic of Fennoscandia as Context for the Fennoscandian Arctic Russia—Drilling Early Earth Project, Frontiers in Earth Sciences*; Melezhik, V.A., Prave, A.R., Fallick, A.E., Kump, L.R., Strauss, H., Lepland, A., Hanski, E.J., Eds.; Springer: Berlin/Heidelberg, Germany, 2012; pp. 289–385.
41. Mitrofanov, F.P.; Bayanova, T.B.; Korchagin, A.U.; Groshev, N.Y.; Malitch, K.N.; Zhironov, D.V.; Mitrofanov, A.F. East Scandinavian and Noril'sk plume mafic large igneous provinces of Pd-Pt ores: Geological and metallogenic comparison. *Geol. Ore Depos.* **2013**, *55*, 305–319. [[CrossRef](#)]
42. Mints, M.V. 3D model of deep structure of the Early Precambrian crust in the East European Craton and paleogeodynamic implications. *Geotectonics* **2011**, *45*, 267–290. [[CrossRef](#)]
43. Mitrofanov, F.P. New Types of Mineral Raw Materials in the Kola Province: Discoveries and Perspectives. In *Smirnovsky Collection of Works*; VINITI RAS: Moscow, Russia, 2005; pp. 39–53.
44. Sharkov, E.V. *Formation of Layered Intrusions and Related Mineralization*; Scientific World: Moscow, Russia, 2006.
45. Zozulya, D.R.; Bayanova, T.B.; Eby, G.N. Geology and Age of the Late Archean Keivy Alkaline Province, Northeastern Baltic Shield. *J. Geol.* **2005**, *113*, 601–608. [[CrossRef](#)]
46. Groshev, N.; Karykowski, B. The Main Anorthosite Layer of the West-Pana Intrusion, Kola Region: Geology and U-Pb Age Dating. *Minerals* **2019**, *9*, 71. [[CrossRef](#)]
47. Grokhovskaya, T.L.; Ivanchenko, V.N.; Karimova, O.V.; Griboedova, I.G.; Samoshnikova, L.A. Geology, mineralogy, and genesis of PGE mineralization in the South Sopcha massif, Monchegorsk complex, Russia. *Geol. Ore Depos.* **2012**, *54*, 347–369. [[CrossRef](#)]
48. Kozlov, E.K. *Natural Series of Nickel-Bearing Rocks and Their Metallogeny*; Nauka: Leningrad, Russia, 1973.
49. Smolkin, V.F.; Mitrofanov, F.P. *Layered Intrusions of the Monchegorsk Ore District: Petrology, Mineralization, and Deep Structure*; Mitrofanov, F.P., Smolkin, V.F., Eds.; Kola Science Center RAS: Apatity, Russia, 2004.
50. Raczek, I.; Jochum, K.P.; Hofmann, A.W. Neodymium and strontium isotope data for USGS reference materials BCR-1, BCR-2, BHV O-1, BHVO-2, AGV-1, AGV-2, GSP-1, GSP-2 and Eight MPI-DING reference glasses. *Geostand. Geoanal. Res.* **2003**, *27*, 173–179. [[CrossRef](#)]
51. Tanaka, T.; Togashi, S.; Kamioka, H.; Amakawa, H.; Kagami, H.; Hamamoto, T.; Yuhara, M.; Orihashi, Y.; Yoneda, S.; Shimizu, H.; et al. JNdi-1: A neodymium isotopic reference in consistency with LaJolla neodymium. *Chem. Geol.* **2000**, *168*, 279–281. [[CrossRef](#)]
52. Ludwig, K.R. Isoplot 3.75. A Geochronological Toolkit for Microsoft Excel. *Berkeley Geochronol. Cent. Spec. Publ.* **2012**, *4*, 71.
53. Bouvier, A.; Vervoort, J.D.; Patchett, P.J. The Lu-Hf and Sm-Nd isotopic composition of CHUR: Constraints from unequilibrated chondrites and implications for the bulk composition of terrestrial planets. *Earth Planet. Sci. Lett.* **2008**, *273*, 48–57. [[CrossRef](#)]
54. Goldstein, S.J.; Jacobsen, S.B. Nd and Sr isotopic systematics of river water suspended material: Implications for crustal evolution. *Earth Planet. Sci. Lett.* **1988**, *87*, 249–265. [[CrossRef](#)]
55. Nitkina, E.A. U-Pb zircon dating of rocks of the platiniferous Fedorova-Pana Layered Massif, Kola Peninsula. *Dokl. Earth Sci.* **2006**, *408*, 551–554. [[CrossRef](#)]
56. Dodson, M.H. Closure temperature in cooling geochronological and petrological systems. *Contrib. Mineral. Petrol.* **1973**, *40*, 259–274. [[CrossRef](#)]
57. Hensen, B.J.; Zhou, B.O. Retention of isotopic memory in garnets partially broken down during an overprinting granulite-facies metamorphism: Implications for the Sm-Nd closure temperature. *Geology* **1995**, *23*, 225–228. [[CrossRef](#)]
58. Mezger, K.; Essene, E.J.; Halliday, A.N. Closure temperatures of the Sm-Nd system in metamorphic garnets. *Earth Planet. Sci. Lett.* **1992**, *113*, 397–409. [[CrossRef](#)]
59. Groshev, N.Y.; Nitkina, E.A.; Mitrofanov, F.P. Two-phase mechanism of the formation of platinum-metal basites of the Fedorova Tundra intrusion on the Kola Peninsula: New data on geology and isotope geochronology. *Dokl. Earth Sci.* **2009**, *427*, 1012–1016. [[CrossRef](#)]
60. Korchagin, A.U.; Goncharov, Y.V.; Subbotin, V.V.; Groshev, N.Y.; Gabov, D.A.; Ivanov, A.N.; Savchenko, Y.E. Geology and Composition of the Ores of the Low-Sulfide North Kamennik PGE Deposit in the West-Pana Intrusion. *Ores Met.* **2016**, *1*, 42–51. (In Russian)
61. Chistyakova, S.; Latypov, R.; Zaccarini, F. Chromitite Dykes in the Monchegorsk Layered Intrusion, Russia: In Situ Crystallization from Chromite-Saturated Magma Flowing in Conduits. *J. Petrol.* **2015**, *56*, 2395–2424. [[CrossRef](#)]
62. Latypov, R.; Costin, G.; Chistyakova, S.; Hunt, E.J.; Mukherjee, R.; Naldrett, T. Platinum-bearing chromite layers are caused by pressure reduction during magma ascent. *Nat. Commun.* **2018**, *9*, 462. [[CrossRef](#)]
63. Chashchin, V.V.; Bayanova, T.B.; Yelizarova, I.R.; Serov, P.A. The Volch'etundrovsky Massif of the autonomous anorthosite complex of the Main Range, the Kola Peninsula: Geological, petrogeochemical, and isotope-geochronological studies. *Petrology* **2012**, *20*, 467–490. [[CrossRef](#)]

64. Kunakkuzin, E.; Borisenko, E.; Nerovich, L.; Serov, P.; Bayanova, T. The Origin and Evolution of Ore-Bearing Rocks in the Loypishnun Deposit (Monchetundra Massif, NE Fennoscandian Shield): Isotope Nd-Sr and REE Geochemical Data. *Minerals* **2020**, *10*, 286. [[CrossRef](#)]
65. Sharkov, E.V.; Smol'kin, V.F.; Belyatskii, V.B.; Chistyakov, A.V.; Fedotov, Z.A. Age of the Moncha Tundra fault, Kola Peninsula: Evidence from the Sm-Nd and Rb-Sr isotopic systematics of metamorphic assemblages. *Geochem. Int.* **2006**, *44*, 317–326. [[CrossRef](#)]
66. Ernst, R.E.; Jowitt, S.M. Large igneous provinces (LIPs) and metallogeny. *Tecton. Metallog. Discov. N. Am. Cordill. Similar Accretionary Settings* **2013**, *17*, 17–51.
67. Steshenko, E.N.; Bayanova, T.B.; Serov, P.A. The Paleoproterozoic Kandalaksha-Kolvitsa Gabbro-Anorthosite Complex (Fennoscandian Shield): New U-Pb, Sm-Nd, and Nd-Sr (ID-TIMS) Isotope Data on the Age of Formation, Metamorphism, and Geochemical Features of Zircon (LA-ICP-MS). *Minerals* **2020**, *10*, 254. [[CrossRef](#)]
68. Jahn, B.M.; Wu, F.; Chen, B. Massive granitoid generation in Central Asia: Nd isotope evidence and implication for continental growth in the Phanerozoic. *Episodes* **2000**, *23*, 82–92. [[CrossRef](#)]
69. Timmerman, M.J.; Daly, J.S. Sm-Nd evidence for late Archaean crust formation in the Lapland-Kola Mobile Belt, Kola Peninsula, Russia and Norway. *Precambrian Res.* **1995**, *72*, 97–107. [[CrossRef](#)]
70. Amelin, Y.V.; Semenov, V.S. Nd and Sr isotopic geochemistry of mafic layered intrusions in the eastern Baltic shield: Implications for the evolution of Paleoproterozoic continental mafic magmas. *Contrib. Mineral. Petrol.* **1996**, *124*, 255–272. [[CrossRef](#)]
71. Puchtel, I.S.; Zhuravlev, D.Z.; Kulikova, V.V.; Samsonov, A.V.; Simon, A.K. Komatiites of the Vodlozero Block, Baltic Shield. *Dokl. USSR Acad. Sci.* **1991**, *317*, 167–172.
72. Wedepohl, H.K. The composition of the continental crust. *Geochim. Cosmochim. Acta* **1995**, *59*, 1217–1232. [[CrossRef](#)]